

ornl



3 4456 0378202 0

ORNL/TM-12500

**OAK RIDGE
NATIONAL
LABORATORY**

MARTIN MARIETTA

FAFCO Ice Storage Test Report

Therese K. Stovall

OAK RIDGE NATIONAL LABORATORY
CENTRAL RESEARCH LIBRARY
CIRCULATION SECTION
4500N ROOM 175

LIBRARY LOAN COPY

DO NOT TRANSFER TO ANOTHER PERSON

If you wish someone else to see this
report, send in name with report and
the library will arrange a loan.

VCN-7969 (3 9-77)

MANAGED BY
MARTIN MARIETTA ENERGY SYSTEMS, INC.
FOR THE UNITED STATES
DEPARTMENT OF ENERGY

This report has been reproduced directly from the best available copy.

Available to DOE and DOE contractors from the Office of Scientific and Technical Information, P.O. Box 62, Oak Ridge, TN 37831; prices available from (615) 576-8401, FTS 626-8401.

Available to the public from the National Technical Information Service, U.S. Department of Commerce, 5285 Port Royal Rd., Springfield, VA 22161.

This report was prepared as an account of work sponsored by an agency of the United States Government. Neither the United States Government nor any agency thereof, nor any of their employees, makes any warranty, express or implied, or assumes any legal liability or responsibility for the accuracy, completeness, or usefulness of any information, apparatus, product, or process disclosed, or represents that its use would not infringe privately owned rights. Reference herein to any specific commercial product, process, or service by trade name, trademark, manufacturer, or otherwise, does not necessarily constitute or imply its endorsement, recommendation, or favoring by the United States Government or any agency thereof. The views and opinions of authors expressed herein do not necessarily state or reflect those of the United States Government or any agency thereof.

ORNL/TM-12500
Dist. Category UC-202

94a

Engineering Technology Division

FAFCO ICE STORAGE TEST REPORT

Therese K. Stovall

Date Published: November 1993

Prepared for the
Electric Power Research Institute
under Interagency Agreement No. DOE ERD-91-1022

Prepared by the
OAK RIDGE NATIONAL LABORATORY
Oak Ridge, Tennessee 37831-6285
managed by
MARTIN MARIETTA ENERGY SYSTEMS, INC.
for the
U.S. DEPARTMENT OF ENERGY
under contract DE-AC05-84OR21400



3 4456 0378202 0

CONTENTS

	<u>Page</u>
LIST OF FIGURES	v
LIST OF TABLES	vii
ABBREVIATIONS AND SYMBOLS	ix
ACKNOWLEDGMENTS	xi
ABSTRACT	1
1. INTRODUCTION	1
2. SYSTEM DESCRIPTION	4
2.1 FAFCO STORAGE SYSTEM	4
2.2 TEST FACILITY	4
3. SYSTEM TESTS	8
4. ANALYSIS METHODOLOGY	9
4.1 DATA PROCESSING	9
4.2 REFRIGERATION EFFECT	10
4.2.1 Storage Tank	10
4.2.2 Refrigeration System	12
4.3 DISCHARGE ENERGY AVAILABLE	14
4.4 SHELL HEAT GAINS	15
5. RESULTS	16
5.1 GENERAL OPERATION	16
5.2 CHARGING PERFORMANCE	16
5.3 DISCHARGE PERFORMANCE	33
5.4 STANDBY HEAT GAINS	40
6. CONCLUSIONS AND RECOMMENDATIONS	42
REFERENCES	43
APPENDIX A: ISTF INSTRUMENTATION	44
APPENDIX B: CMA TESTS IN FAFCO TANK	47

LIST OF FIGURES

Figure		Page
1	ISTF schematic for FAFCO storage system	5
2	Summary of FAFCO charge tests	17
3	Capacity variation during FAFCO charge tests, based on brine flow rate and temperature change in the ice tank	19
4	Ice storage capacity measured during FAFCO charge tests	20
5	FAFCO inlet brine temperatures during repetitive series of charge tests	21
6	FAFCO inlet brine temperatures show difference between initial and succeeding charge tests	22
7	Effect of pre-test conditions on tank water level indicator	23
8	Effect of brine flow rate on tank inlet temperature during FAFCO charge tests	24
9	Variation in average (of inlet and outlet) brine temperature during FAFCO charge tests over a range of brine flow rates	25
10	Brine inlet temperature affected by charging rate during FAFCO charge tests	26
11	Brine inlet temperature profile vs. cumulative energy storage during FAFCO charge tests	28
12	Typical chiller/condensing unit performance curves	29
13	Graphical depiction of Eqs. (16) and (17) of the relations between charging rate, brine inlet temperature, and tank state of charge for a brine flow rate of 100 gpm	30
14	FAFCO charge test data for brine flow rates between 78 and 125 gpm showing relationship between charging rate, brine inlet temperature, and tank state of charge	31

LIST OF FIGURES (continued)

Figure		Page
15	Intersection of chiller performance and storage system performance parameters	32
16	Ice tank outlet temperature variation for constant discharge rate of 19 tons with controlled tank inlet temperature from 50 to 60°F	35
17	Ice tank outlet temperature variation for constant discharge rate of 25 tons with controlled tank inlet temperatures from 50 to 60°F.	36
18	Ice tank outlet temperature variation for constant discharge rate of 35 tons with controlled inlet temperature of 55 and 60°F	37
19	Available discharge energy vs. time for loads from 19 to 35 tons and a maximum brine temperature of 48°F with controlled heater temperatures	39
20	Available discharge energy vs. time for maximum brine temperature from 40 to 52°F and a load of 25 tons with controlled heater temperatures	40
21	Available discharge energy vs. time for maximum brine temperatures from 40 to 52°F for constant brine flow to the ice tank	41

LIST OF TABLES

Table		Page
1	ISTF monitoring points for the FAFCO brine coil system	6
2	FAFCO charge test summary	18
3	FAFCO charge sizing table, brine flow rates (gpm)	27
4	FAFCO discharge test summary	34

ABBREVIATIONS AND SYMBOLS

Cap _h	discharge capacity measured at heater
Cap _i	discharge capacity measured at ice tank
c _p	specific heat
FE1	refrigerant mass flow to the expansion valves
FE3	brine flow to ice tank
FE4	brine flow from the evaporator
FE5	refrigerant volumetric flow to the condenser
FE6	water flow rate
gpm	gallons per minute
HE1	refrigerant enthalpy entering the condenser
HE2	refrigerant enthalpy leaving the condenser
HE10	enthalpy corresponding to the measured suction temperature and pressure of the superheated refrigerant leaving the chiller/evaporator
ISTF	Ice Storage Test Facility
PDE1	tank water depth
\dot{Q}_c	heat of rejection predicted by the compressor manufacturer
\dot{Q}_r	heat rejected by the refrigerant
\dot{Q}_w	heat absorbed by the cooling water
Re _b	refrigeration effect as determined by measured brine flow rate and temperature change at ice storage tank
Re _c	refrigeration capacity predicted by the capacity curves
RE _{fch}	refrigeration effect as determined by measured refrigerant flow rates and thermodynamic properties
SC	state of charge
SG	specific gravity
T	temperature
TE2	condenser discharge temperature
TE11	brine temperature entering heater

TE12	brine temperature leaving heater
TE15	brine temperature leaving the ice tank
TE16	brine temperature entering the ice tank
TE17	brine temperature leaving the chiller/evaporator
TE18	brine temperature entering the chiller/evaporator
TE19	water temperature exiting the condenser
TE20	water temperature into the condenser
T_d	saturated discharge temperature
T-h	ton-hour
T_s	saturated suction temperature
\dot{W}_c	compressor power predicted by the manufacturer's data
VE1	refrigerant specific volume entering the condenser
ρ	density
τ	time

ACKNOWLEDGMENTS

This important research has been made possible by the support of the Electric Power Research Institute. I would like to thank the program manager, Ronald Wendland, for his critical support and enthusiasm. FAFCO, Inc. provided the unit for testing. John Tomlinson of Oak Ridge National Laboratory designed the Ice Storage Test Facility, supervised its construction, and has provided valuable guidance during the testing process. Delmar Fraysier is the chief operator of the test facility and made important contributions to the test procedures.

FAFCO ICE STORAGE TEST REPORT*

Therese K. Stovall

ABSTRACT

The Ice Storage Test Facility (ISTF) is designed to test commercial ice storage systems. FAFCO provided a storage tank equipped with coils designed for use with a secondary fluid system. The FAFCO ice storage system was tested over a wide range of operating conditions. Measured system performance during charging showed the ability to freeze the tank fully, storing from 150 to 200 ton-h. However, the charging rate showed significant variations during the latter portion of the charge cycle. During discharge cycles, the storage tank outlet temperature was strongly affected by the discharge rate and tank state of charge. The discharge capacity was dependent upon both the selected discharge rate and maximum allowable tank outlet temperature. Based on these tests, storage tank selection must depend on both charge and discharge conditions. This report describes FAFCO system performance fully under both charging and discharging conditions. While the test results reported here are accurate for the prototype 1990 FAFCO Model 200, currently available FAFCO models incorporate significant design enhancements beyond the Model 200. At least one major modification was instituted as a direct result of the ISTF tests. Such design improvements were one of EPRI's primary goals in founding the ISTF.

1. INTRODUCTION

Commercial air-conditioning loads are a large component of the afternoon peak loads served by electric utilities. Increased use of cool storage would shift this electrical load from peak to off-peak periods. This shift would permit utilities to defer construction of additional generating capacity and reduce customers' demand charges.

Although the number of cool storage installations in commercial buildings is growing, it represents only a small fraction of the potential market. One major barrier to the use of

*Units used throughout this report are common to and exclusive in the industry.

cool storage equipment has been the uncertainty associated with its performance. Uniform testing by an independent agency has not been available. The performance data available from manufacturers are varied in scope and detail from one type of device to another and across manufacturers as well. Often system performance values are given for only one operating point, making it difficult to predict performance under other operating conditions.

The Electric Power Research Institute (EPRI) therefore sponsored the development of an Ice Storage Test Facility (ISTF) in 1985 to permit uniform testing of commercial-size cool storage equipment of many different types. This testing serves two purposes: (1) to provide uniform performance test results and (2) to promote system improvements based on experimental data. Uniform test results will be useful to utilities in promoting their installation and use and in requesting rate incentives from public utilities commissions (PUCs) and to building designers in specifying appropriate equipment for their applications. The experimental data will also be useful to equipment designers because it will describe component behavior as well as overall system performance. The capacity of the ISTF was sized at 250 ton-h, large enough to test most commercially available units. Real-time data acquisition and precise computer controls were included.

The ISTF can be used to test dynamic, liquid recirculation, secondary fluid, and direct expansion (DX) ice makers. The simplest ice maker is a DX machine. In a DX ice maker, the refrigerant is sent as a cold liquid into coils submerged in a tank of water. As the refrigerant passes through these coils, it absorbs heat from the water and evaporates. As the refrigerant leaves the coils, it is completely gaseous and usually slightly superheated. The water in the tank is thereby chilled until it becomes frozen. When the stored cooling is needed, the ice is melted by circulating warm water from the heat load through the ice and returning the chilled water to the heat load. This arrangement is called an exterior melt because the ice is melted from the surface opposite from where it is formed.

In a secondary fluid system, the cold liquid refrigerant is sent to a heat exchanger outside the tank of water. In this heat exchanger, a secondary fluid, typically a glycol mixture, is chilled. This secondary fluid is then sent to the tank of water where it absorbs

heat from the water, again freezing the water in the tank. The secondary fluid can also be used to transfer the stored cooling to the heat load. This arrangement is called an internal melt. The stored cooling energy can also be transferred to the heat load by using an external melt as described for the DX system.

A liquid recirculation system is similar to the DX system because the cold refrigerant is sent to coils submerged in the tank of water. However, in the liquid recirculation system, the amount of refrigerant circulated through the coils is typically two to three times greater than in a DX system so that only a portion of the refrigerant is evaporated and the coils remain full of liquid throughout their length. This additional refrigerant circulation is accomplished through the use of gravity feed or a refrigerant pump. The stored cooling energy is transferred to the heat load using an external melt arrangement.

A dynamic ice maker freezes ice using either a DX or a liquid overfeed arrangement. However, in a dynamic system, the ice is harvested on a periodic basis by a defrosting cycle. This harvesting cycle reduces the ice thickness on the heat transfer surface of the chiller. After the ice is harvested, it is stored in a slush or slurry of ice and water. The water is circulated to provide the stored cooling to the heat load.

This report describes the test results for an ice storage tank furnished by the FAFCO, Inc. The FAFCO storage tank is both charged and discharged using a secondary fluid or brine. The storage system and the test facility are described in Sect. 2. Section 3 describes the tests that were performed to characterize the storage system, and Sect. 4 describes the analysis methods used to evaluate the performance data. The results and recommendations are summarized in Sects. 5 and 6.

2. SYSTEM DESCRIPTION

2.1 FAFCO STORAGE SYSTEM

The 1990 FAFCO model 200 ice tank is chilled by the flow of brine through 1/4-in.-OD plastic tubing, arranged in 24 separate heat exchangers within the tank. These tubes are almost completely submerged in water. The brine used for these tests was a mixture of ethylene glycol and water with a freezing point of -0°F . The FAFCO ice tank is discharged by circulating the brine through the tank and then through the desired heat load, simulated by a simple heater in the test facility. The FAFCO unit is equipped with a water depth sensor that can be used to infer the amount of ice stored during a charging cycle and the state of charge during a discharge cycle.¹

The FAFCO tank was filled with the specified volume of 2367 gal of water and the level indicator zero level was adjusted. The volume of brine in the storage system coils was estimated to be 105 gal., based on the amount of brine pumped into the tank and the nearby piping.

While the test results reported here are accurate for the prototype 1990 FAFCO Model 200, currently available FAFCO models incorporate significant design enhancements beyond the Model 200. At least one major modification was instituted as a direct result of the ISTF tests. As described earlier, such design improvements were one of EPRI's primary goals in founding the ISTF.

2.2 TEST FACILITY

The test facility was designed to test a wide variety of storage systems. It includes all refrigeration system components necessary to charge brine systems. Figure 1 shows the test facility configuration used to test the FAFCO storage tank equipped with the brine coils. The test facility is well-equipped with monitoring devices to measure temperature, pressure, flow, and energy use. The monitoring points shown in Fig. 1 are listed in Table 1. A clear plastic tube was attached to the FAFCO level indicator and to a differential pressure

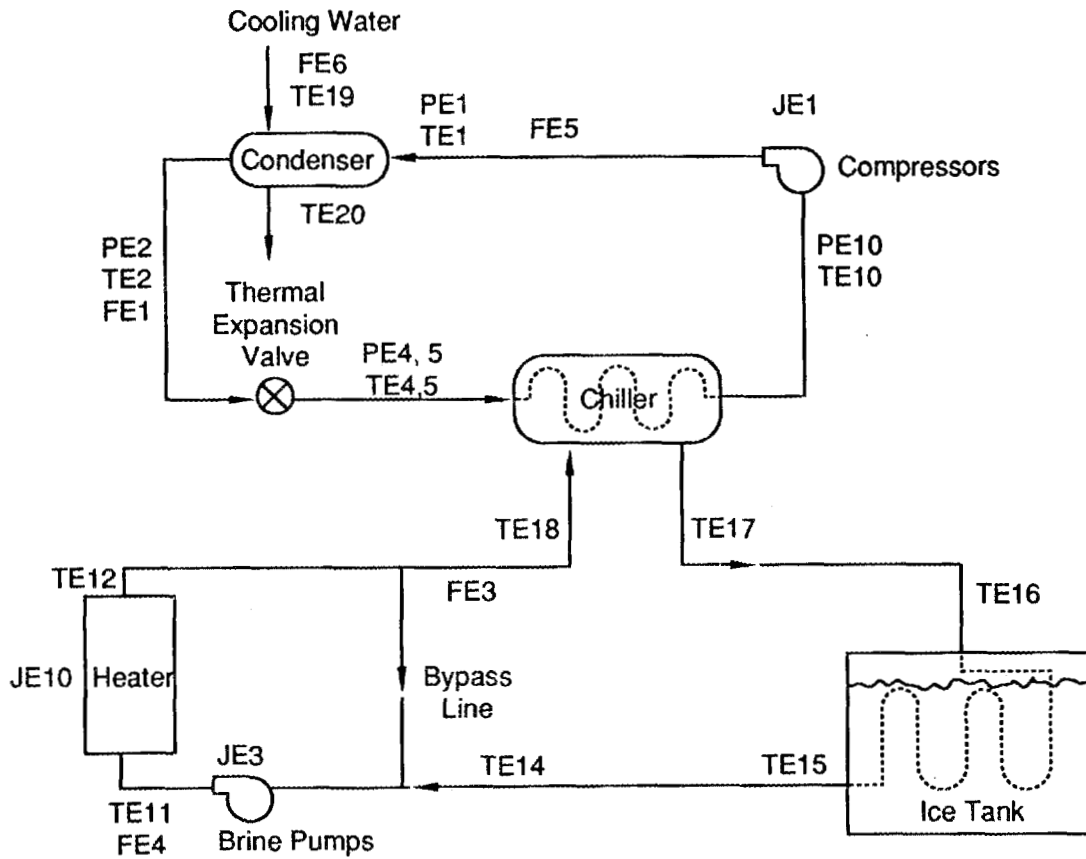


Fig. 1. ISTF schematic for FAFCO storage system.

monitoring device to allow the continuous recording of the tank's water level. The measured water level reflects changes in the tank water depth that occur during freezing due to the difference in density between ice and water. The test loop instrumentation is described more fully in Appendix A and Ref. 2.

A variable speed pump was used to circulate brine during both the charge and discharge cycles, as is shown in Fig. 1. The evaporator/chiller (see Fig. 1) connects the test facility's refrigeration system to the brine loop that charges the ice storage tank. In the

Table 1. ISTF monitoring points
for the FAFCO brine coil system

Point label	Measured quantity
FE1	Chiller inlet flow, refrigerant, mass
FE3	Chiller inlet flow, brine
FE4	Brine pump discharge flow
FE5	Compressor outlet flow, volume
FE6	Condenser inlet water flow
JE1	Compressor energy and power
JE3	Brine pump energy and power
JE10	Heater energy and power
PE1	Compressor discharge pressure
PE2	Condenser outlet refrigerant pressure
PE4	Chiller inlet refrigerant pressure
PE5	Chiller inlet refrigerant pressure
PE10	Compressor suction pressure
TE1	Compressor discharge temperature
TE2	Condenser discharge temperature
TE4	Chiller inlet refrigerant temperature
TE5	Chiller inlet refrigerant temperature
TE10	Compressor suction temperature
TE11	Heater inlet water temperature
TE12	Heater outlet water temperature
TE14	Ice tank outlet brine temperature
TE15	Ice tank outlet brine temperature
TE16	Ice tank inlet brine temperature
TE17	Chiller outlet brine temperature
TE18	Chiller inlet brine temperature
TE19	Condenser inlet water temperature
TE20	Condenser outlet water temperature

evaporator/chiller, a refrigerant is vaporized, absorbing heat from the brine. To accommodate the desired wide range of testing conditions, a chiller with two independent and equal-size refrigerant coils was selected. The control system is designed to select one or both chiller coils based on the compressor loading. The thermal expansion valves feeding refrigerant to these coils open and close in response to the measured superheat at the coil exit. Because the evaporator/chiller was often running under part-load conditions, the

thermal expansion valves exhibited a large degree of hunting during the beginning of most freeze tests. This is typical for part-loaded expansion valves, and the hunting usually stopped after ~30 to 45 min of operation. The brine pump speed was varied to control the brine flow rate at the selected value during the charge cycle.

Two parallel compressors with part-load capabilities are used to vary the chiller capacity from 15 to 95 tons. The flow of water to the condenser controls the condensing temperature between 80 and 100°F. During discharge cycles, the brine pump speed, heater power, and bypass valve positions are used to control test conditions.

3. SYSTEM TESTS

The test plan was structured to test the storage tank's capabilities under a wide range of operating conditions. The charging tests were designed to determine how the storage system would respond to ice-charging periods from 8 to 16 h and brine flow rate from 50 to 150 gal/min. The ice-discharge tests mimicked discharge periods ranging from 6 to 12 h with varying temperature and flow requirements at the heater. A series of tests were made under repetitive conditions to simulate conditions that might be found in a commercial application. The test results were questioned because the temperature measurement accuracy of $\pm 0.5^{\circ}\text{F}$ often represented a significant fraction of the temperature change in the heat exchanger. Therefore this series was repeated after the temperature measuring devices at the ISTF were upgraded to a tolerance of $\pm 0.2^{\circ}\text{F}$. This second series of tests gave the same results as the first series.

Ice tank heat gains were measured by recording the change in ice inventory over a long period of time in the absence of all external fluid flows. The ice depletion over this time period was ascribed to shell heat gains. The ambient temperature was noted during the standby test. Because of the sheltered location of the test floor, the ambient conditions showed little variation.

In addition to the performance tests, tests were also made using an experimental salt that prior tests had shown would serve as an aid to ice-shedding for dynamic ice makers. This salt affected the freezing temperature of the water as well as the structure of the ice crystals. These tests are described in Appendix B.

4. ANALYSIS METHODOLOGY

The primary concern of the data analysis is to produce useful information and to present it in a meaningful fashion. Another concern is to distinguish between the performance of the ice storage system and the performance of the refrigeration system. While analysis of the refrigeration system performance can prove enlightening and is certainly useful to system designers, it must be distinguished from that of the manufacturer's storage system. Also, the test facility is different from a commercial system because it must have the flexibility to test a wide variety of system types. This introduces added complexity that a commercial system would not encounter.

4.1 DATA PROCESSING

The data available for each operational test permit redundant calculations that increase our understanding and confidence in the test results. For example, the heat rejection at the condenser is measured on both the water and refrigerant sides of the heat exchanger. The refrigeration effect to the ice tank is measured by both changes in the water height (a measure of the ice inventory) and by the brine flow and temperature change. The refrigeration effect is also measured at the chiller on both the brine and refrigerant sides. The energy available for discharge is measured by brine flow and temperatures at the heater and at the ice tank, as well as by the power going to the discharge heater. This duplication of measurements also enables us to more fully separate the performance of the ice storage system from that of the refrigeration system.

The data are collected for each monitoring point every 30 s. This collection frequency is dictated by system control requirements rather than by the analysis requirements. The data are immediately summed (for flows or energy uses) or averaged (for temperatures, pressures, power uses, and flow rates) to represent the appropriate values on a 5-min basis.

Thermodynamic properties for R-22 are calculated from a computerized format developed by G. T. Kartsounes and R. A. Erth and adapted for use at Oak Ridge National Laboratory (ORNL) by C. K. Rice and S. K. Fischer.³ Brine properties, as a function of concentration and temperature, were provided by Union Carbide Corporation, and information for the temperature range of interest was extracted.⁴

4.2 REFRIGERATION EFFECT

4.2.1 Storage Tank

The refrigeration effect (or stored cool) in the ice tank is directly measured by recording the depth of the water in the tank. This measurement is reliable when ice is present in the tank and when the ice is submerged, conditions that occur for this unit only during a charging cycle following a complete melt. The measured density of ice in previous local tests was 57.2 lb/ft³, in good agreement with the reported range of 57.2 lb/ft³ at 0°C to 57.4 lb/ft³ at -10°C (Ref. 5). The measured volume change vs tank depth change above the fully filled/fully melted level was 38.8 gal/in. (195 gal./5.02 in.). These figures, combined with an assumed water density of 62.4 lb/ft³ and the heat of fusion of 144 Btu/lb, produce a latent storage capacity of 40.8 ton-h/in. change in water depth.

The stored cooling effect is also calculated from the measured brine flow rate and temperature gain as is shown in Eq. (1).

$$RE_b = FE4 \times c_p \times \rho \times (TE15 - TE16) , \quad (1)$$

where

- RE_b = refrigeration effect produced by the brine,
- $FE4$ = brine flow from the chiller,
- c_p = brine specific heat,
- ρ = brine density,

- TE15 = brine temperature leaving the ice tank, and
 TE16 = brine temperature entering the ice tank.

The brine specific heat and specific gravity are provided in the form of families of curves in Ref. 4. Interpolations from these curves for the temperature range from 20 to 60°F and a brine concentration of 33 wt % produced the following equations for specific gravity (relative to water at 60°F) and specific heat.

$$SG = -0.0002 \times T + 1.063 \quad , \quad (2)$$

and,

$$c_p = 0.0003 \times T + 0.899 \quad , \quad (3)$$

where

- SG = specific gravity,
 T = average brine temperature (°F), and
 c_p = specific heat [Btu/(lb-°F)].

Interpolation for a brine concentration of 25 wt % produced Eqs. (4) and (5).

$$SG = -0.000108 \times T + 1.0482 \quad , \quad (4)$$

$$c_p = 0.000275 \times T + 0.922 \quad . \quad (5)$$

The system capacity was also measured at the evaporator/chiller, on both the brine and refrigerant sides. These measurements provide another checkpoint to guard against instrument failure. The capacity measured at the chiller is expected to be slightly higher than that at the ice tank due to shell heat gains at the tank and in the piping and also by the amount of energy added by the brine pumps. The brine-side measurements are similar to

those used for the ice tank and are shown in Eq. (6). The refrigerant-side measurements are used in Eq. (7). Shell losses from the well-insulated chiller are assumed to be negligible.

$$RE_{bch} = FE4 \times \rho \times c_p \times (TE18 - TE17) , \quad (6)$$

where

- RE_{bch} = refrigeration effect at the chiller, based on brine flow and temperature measurements,
- $FE4$ = brine flow from the chiller,
- c_p = brine specific heat,
- ρ = brine density,
- $TE17$ = brine temperature leaving the chiller, and
- $TE18$ = brine temperature entering the chiller.

$$RE_{fch} = FE1 \times (HE10 - HE2) , \quad (7)$$

where

- RE_{fch} = refrigeration effect at the chiller, based on refrigerant flow and property measurements,
- $FE1$ = refrigerant flow to the chiller,
- $HE10$ = enthalpy corresponding to the measured suction temperature and pressure of the superheated refrigerant leaving the chiller, and
- $HE2$ = enthalpy corresponding to the saturated liquid refrigerant leaving the condenser.

4.2.2 Refrigeration System

Another measurement of the system capacity can be taken from the compressor curves. These curves were modeled by Eqs. (8), (10), and (11). Equation (8) predictions match the compressor manufacturer's table within ± 0.5 ton. Equation (9) is taken directly from the manufacturer's literature. Equation (10) predictions match the manufacturer's table within ± 0.5 hp. The heat of rejection model, Eq. (11), matched the manufacturer's table

within ± 0.02 ton. Many tests were run at part-load conditions; that is, the compressor was not operating at full capacity. The compressor capacity and heat rejection predictions were therefore reduced in proportion to the loading on the compressor. The manufacturer's power consumption table is good only for fully loaded conditions and cannot accurately predict part-load power requirements.

$$\begin{aligned} \text{Re}_c = & 49.35 + 1.663 \times T_s - 0.00173 \times T_d^2 - 0.00708 \times T_s \times T_d \\ & + 0.00953 \times T_s^2 \times C_s, \end{aligned} \quad (8)$$

$$C_s = 1 + 0.0005 \times (T_d - \text{TE2} - 15), \quad (9)$$

$$\begin{aligned} \dot{W}_c = & 44.088 - 0.508 \times T_s + 0.000840 \times T_d^2 + 0.0123 \times T_s \times T_d \\ & - 0.00592 \times T_s^2, \end{aligned} \quad (10)$$

$$\dot{Q}_c = 1.090 - 0.00422 \times T_s + 0.00263 \times T_d, \quad (11)$$

where

Re_c = refrigeration capacity predicted by the compressor capacity curves (tons),

T_s = saturated suction temperature ($^{\circ}\text{F}$),

T_d = saturated discharge temperature ($^{\circ}\text{F}$),

C_s = capacity correction for subcooling (table based on 15°F),

TE2 = condenser discharge temperature,

\dot{W}_c = compressor power predicted by the manufacturer's data (bhp), and

\dot{Q}_c = heat of rejection predicted by the compressor manufacturer (ton).

As another check on the system, the heat rejected at the condenser is measured on both the refrigerant and water sides [see Eqs. (12) and (13)].

$$\dot{Q}_w = FE6 \times \rho \times c_p \times (TE20 - TE19) , \quad (12)$$

$$\dot{Q}_r = \frac{FE5}{VE1} \times (HE1 - HE2) , \quad (13)$$

where

- \dot{Q}_w = heat absorbed by the cooling water,
- FE6 = water flow rate,
- c_p = specific heat of water,
- TE20 = water temperature into the condenser,
- TE19 = water temperature exiting the condenser,
- \dot{Q}_r = heat rejected by the refrigerant,
- FE5 = refrigerant volume flow entering the condenser,
- VE1 = refrigerant specific volume entering the condenser,
- HE1 = refrigerant enthalpy entering the condenser,
- HE2 = refrigerant enthalpy leaving the condenser, and
- ρ = density of water.

4.3 DISCHARGE ENERGY AVAILABLE

The cool storage available to meet a cooling load was measured by the brine flow rates and temperature changes at the heater and at the ice tank [see Eqs. (14) and (15)]. The tank storage inventory is not measurable during the discharge cycle because there is no way of measuring the mixed temperature of the liquid water within the storage tank.

$$cap_h = FE4 \times \rho \times c_p \times (TE12 - TE11) , \quad (14)$$

$$\text{cap}_i = \text{FE3} \times \rho \times c_p \times (\text{TE15} - \text{TE16}) \quad , \quad (15)$$

where

- cap_h = discharge capacity measured at the heater,
- FE4 = brine flow to heater,
- TE12 = brine temperature leaving heater,
- TE11 = brine temperature entering heater,
- c_p = specific heat of brine,
- cap_i = discharge capacity measured at the ice tank,
- FE3 = brine flow to ice tank,
- TE15 = brine temperature leaving ice tank,
- TE16 = brine temperature to ice tank, and
- ρ = brine density.

The heater power was also measured but is considered to be less accurate than the other available measurements, as is discussed in Appendix A. The tank was considered to be fully discharged when it was no longer possible to maintain the desired heater outlet temperature. Some ice may remain in the tank at that time but is unavailable to meet the load.

A few tests were made at a constant brine flow rate through the heater and ice tank, i.e. the brine temperatures at the heater were not controlled. For these tests, the tank was considered fully discharged when the tank outlet temperature exceeded 48°F.

4.4 SHELL HEAT GAINS

Shell heat gains were measured directly from changes in tank water depth over extended periods of time when there was no external flow.

5. RESULTS

5.1 GENERAL OPERATION

The brine pressure drop across the FAFCO coils was measured at flow rates of 25, 50, 75, 100, 125, 150, and 163 gal/min. The measured pressure drop ranged from 0.3 psi at 25 gal/min to 4.7 psi. at 163 gal/min. These values were taken at a brine temperature of 65°F and a concentration of 33%. FAFCO curves show the predicted pressure drop to vary from essentially 0 at 25 gal/min to ~3.8 psi at 163 gal/min. A friction factor correlation shows that the pressure drop is approximately proportional to the Reynold's number raised to the -0.25 power.⁶ Based on this correlation, pressure losses at the recommended brine concentration of 25 wt % should be ~5% less than the measured values and produce pressure drops somewhat closer to the values reported by FAFCO.

FAFCO offers an inventory meter for use in monitoring the ice in the tank. This works by measuring the increase in tank water height that occurs when ice (with a lower density than the surrounding water) is formed. The FAFCO inventory meter was compared to the ISTF differential pressure meter and to a sight tube. The three measurements agreed within $\pm 5\%$, and were usually much closer. The voltage output of the probe was found to be linearly proportional to the tank height during an initial fill test. However, during the testing program, we found that a large amount of ice was usually hung on the tubing above the water level. The only times the water level was able to give a true reading on the amount of ice available within the tank was therefore during the initial charge test and during charge tests that followed 100% discharges (not typical of common practice). FAFCO addressed this problem with design modifications to the Ice Stor units.

5.2 CHARGING PERFORMANCE

When designing a thermal storage system for a given application, the heat rejection temperature, storage capacity, and time available for charging are usually known.⁷ This establishes the average capacity needed during the charging cycle. The ability of a storage

system to meet these requirements is a function of both the storage tank/coil design and of the balance of the refrigeration system, most importantly the compressor. A large number of tests were made to measure the FAFCO Ice Stor charging performance. These tests are summarized in Table 2.

Compressor manufacturers present their capacity as a function of saturated suction and discharge temperatures (Sect. 4.2 described the manufacturer's data for the ISTF compressor). When charging an ice-on-coil storage tank, the suction temperature gradually drops as the water in the tank becomes colder and ice builds up on the coils. The reduced suction temperature leads to a reduced refrigeration capacity. The temperature profile of the fluid entering the tank throughout the charge cycle is therefore an important characteristic of the storage system. Figure 2 shows this temperature profile for many of the FAFCO

ORNL-DWG 93-6577

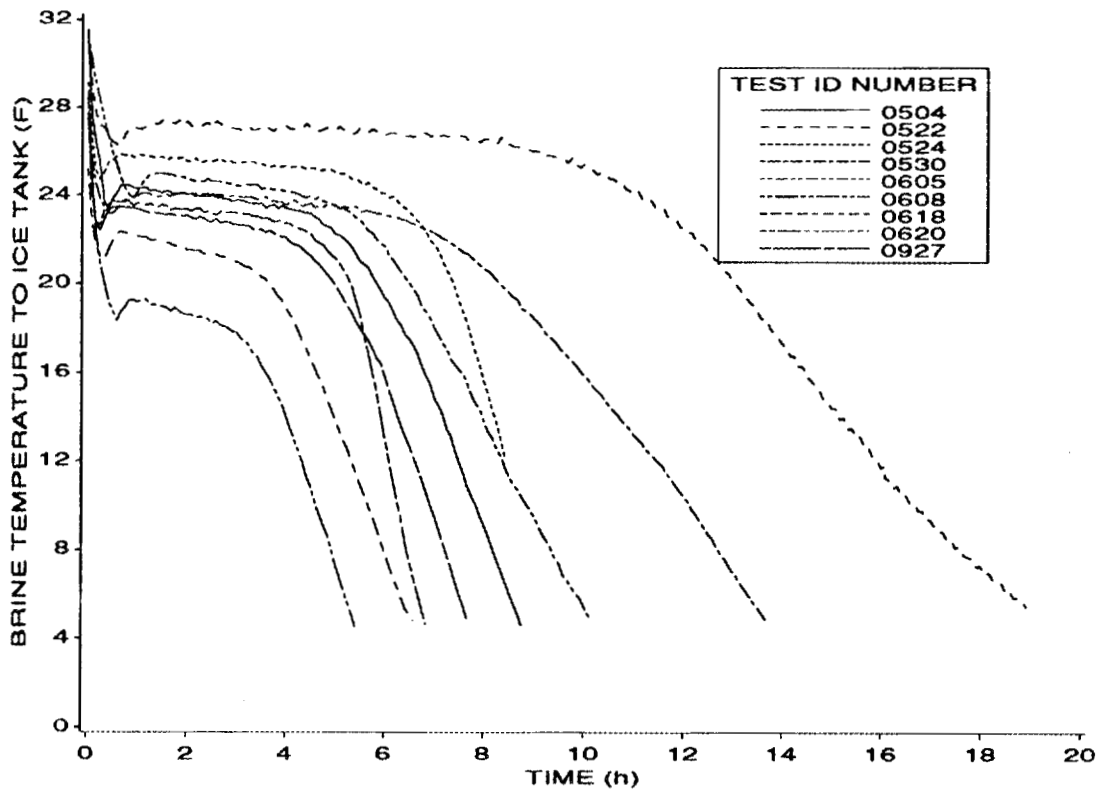


Fig. 2. Summary of FAFCO charge tests.

Table 2. FAFCO charge test summary

ID NUMBER	AVERAGE CHARGING RATE ^a (ton)	TOTAL CHARGE ^b (ton-h)	BRINE FLOW RATE (gpm)	BRINE TEMPERATURE TO TANK		BRINE TEMP. CHANGE IN ICE TANK ^c (°F)	PUMP ENERGY (ton-h)
				AVG (°F)	MIN (°F)		
0327	18	198 ^d	102	21.7	5.1	4.2	8
0416	12	210 ^d	155	19.2	5.7	1.5	30
0426	17	186 ^d	117	19.8	5.3	2.9	11
0430	18	149	119	20.3	5.3	3.3	7
0502	18	150	119	20.2	5.3	3.1	7
0504	18	154	118	20.1	5.1	3.2	7
0516	19	143	48	16.5	10.4	9.8	1
0522	8	160	79	21.6	5.4	2.3	6
0524	15	126	108	23.7	12.2	3.5	5
0530	13	177	60	19.3	5.2	5.5	3
0601	16	158	50	17.5	5.2	8.4	1
0605	18	182 ^d	155	20.0	5.1	2.5	25
0608	30	164	123	16.3	5.1	4.8	8
0613	14	219 ^d	105	19.2	5.1	3.4	10
0618	26	170	150	17.8	5.1	3.6	16
0620	20	136	107	20.7	5.3	4.6	5
0622	25	203 ^d	106	18.6	5.2	5.4	35
0627	20	223 ^d	153	20.0	5.1	2.7	25
0921	19	189 ^d	116	19.0	5.2	3.2	10
0925	19	150	116	19.3	5.1	3.1	9
0927	19	144	116	19.5	5.5	3.2	8
1001	25	137	74	15.2	7.2	8.3	2

^a from brine flow rate and temperature change at ice tank

^b tests covers period when TE16 \leq 32°F

^c RTD specifications $\pm 0.5^\circ\text{F}$ for tests 0327-0627; $\pm 0.2^\circ\text{F}$ for later tests

^d test began in a fully-melted tank

charge tests. Each test profile shares the same basic shape including a small subcooling dip at the beginning of the ice-making period, a plateau as the ice builds on the tubes, and a drop in temperature as the tank reaches the fully frozen state. Note that the lower charging temperatures correspond to the shorter, i.e. faster, tests.

Capacity calculations were described in Sect. 4.2 and are based on an energy balance on the ice tank. As the brine temperature drops as shown in Fig. 2, the capacity of the system also drops as can be seen in Fig. 3. These capacity profiles closely parallel the brine temperature profiles, showing the same level plateau throughout most of the charge cycle followed by a sharp drop in capacity as the tank becomes fully frozen. The cumulative stored energy can be calculated from brine flow and temperature change by summing the capacity throughout the course of the charge test. Figure 4 shows this cumulative stored

ORNL-DWG 93-6578

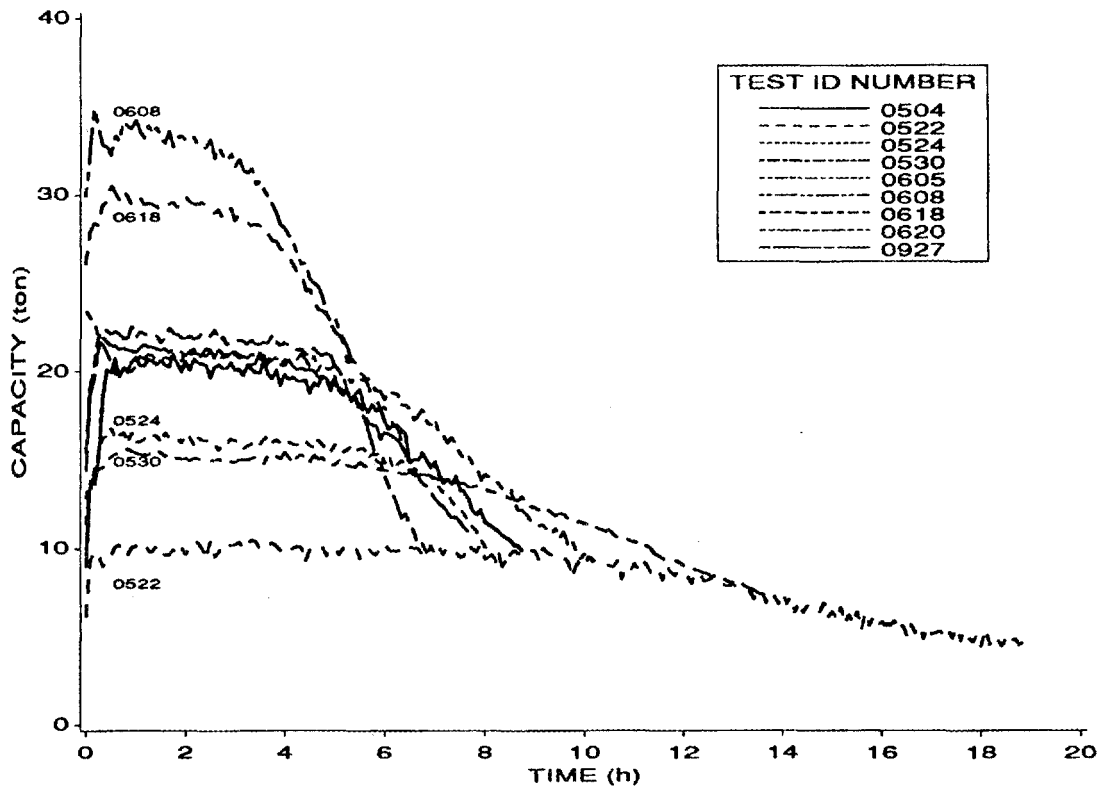


Fig. 3. Capacity variation during FAFCO charge tests, based on brine flow rate and temperature change in the ice tank.

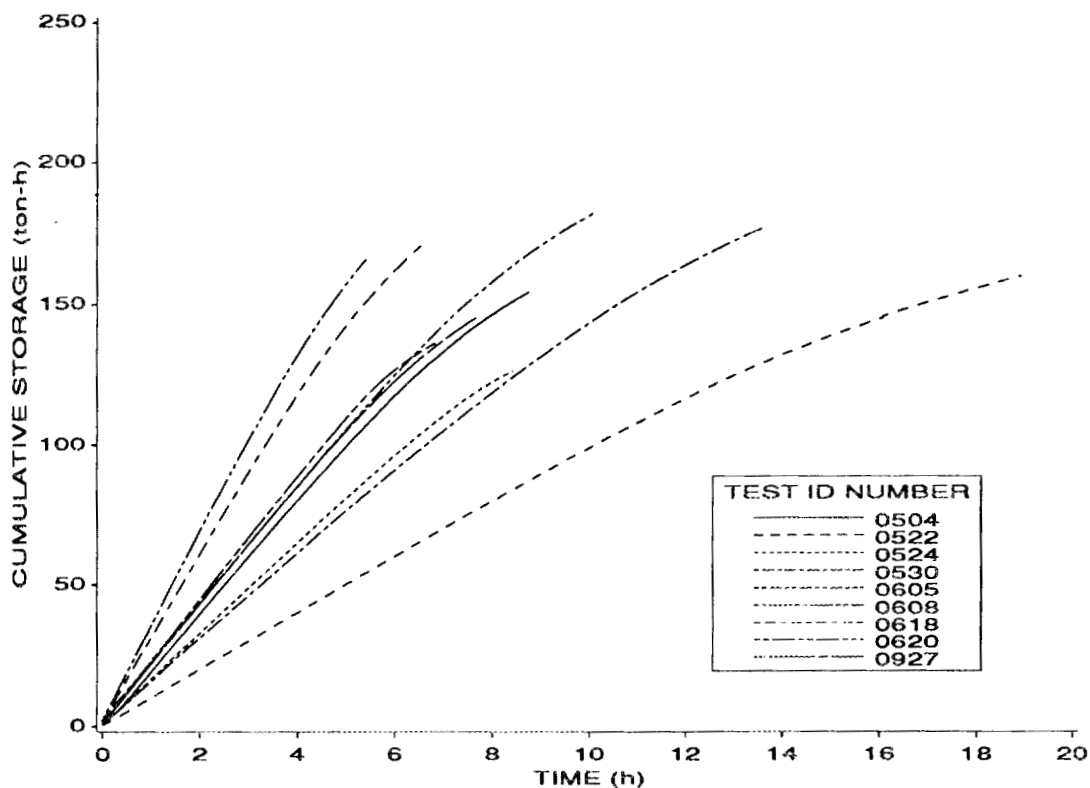


Fig. 4. Ice storage capacity measured during FAFCO charge tests.

energy for most of the charge tests. Those tests included in Fig. 4 were made following a discharge cycle that was stopped when the brine leaving the ice tank could no longer effectively cool the simulated load. Therefore, there is some ice present in the tank at the beginning of the charge cycle. The difference between charging from a fully melted tank and a partially frozen tank can be seen most clearly in Figs. 5 and 6. These figures represent a series of charge and discharge tests made under the same conditions of ~120 gal/min. and ~20 tons. The first test, with test ID number 0426, began with a fully melted tank and takes almost 3 hours longer than the subsequent charge tests, which began from a partially frozen state, and an additional 50 ton-h, or one third more charging energy. After this initial charge however, the system settles out into a steady, repeatable pattern. As mentioned before, the level indicator is only partially useful as an indicator of tank charge. This can be seen in Fig. 7 which shows these same charge tests and the tank water level that

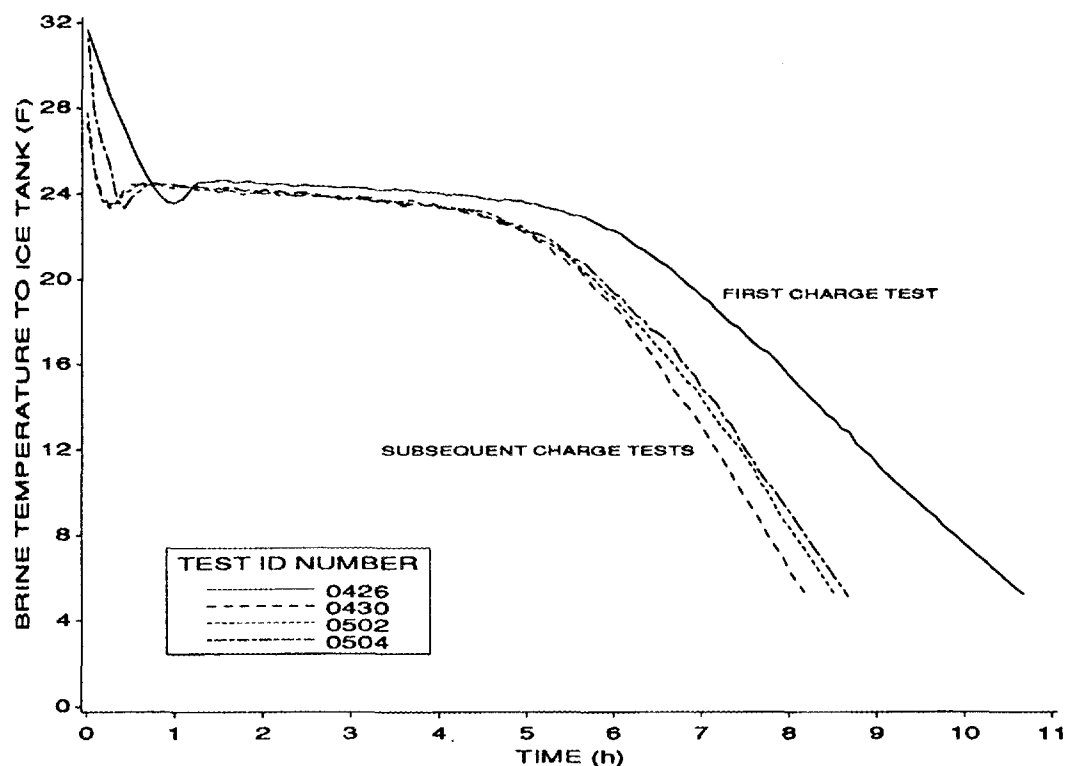


Fig. 5. FAFCO inlet brine temperatures during repetitive series of charge tests.

was measured throughout the tests. Although the amount of energy stored in the tank was ~150 ton-h for each of the three latter tests, the level indicator showed a broader spread in both beginning and ending points. It also shows that the initial test appeared to be less than fully charged, even though this test charged almost 200 ton-h. However, after the initial test, the ending of each test becomes more predictable because most of the ice is eventually submerged as the tank becomes more fully frozen. Therefore, although the level indicator is unreliable as a measure of charge at the beginning and during the course of a charge, it can be used to help determine the presence of a full charge.

As expected, the tests that were run at a higher capacity show the lowest brine temperatures in Figs. 2 and 3. However, the brine flow rate is also an important parameter in determining the brine temperature. Figure 8 shows the variation in brine inlet temperature

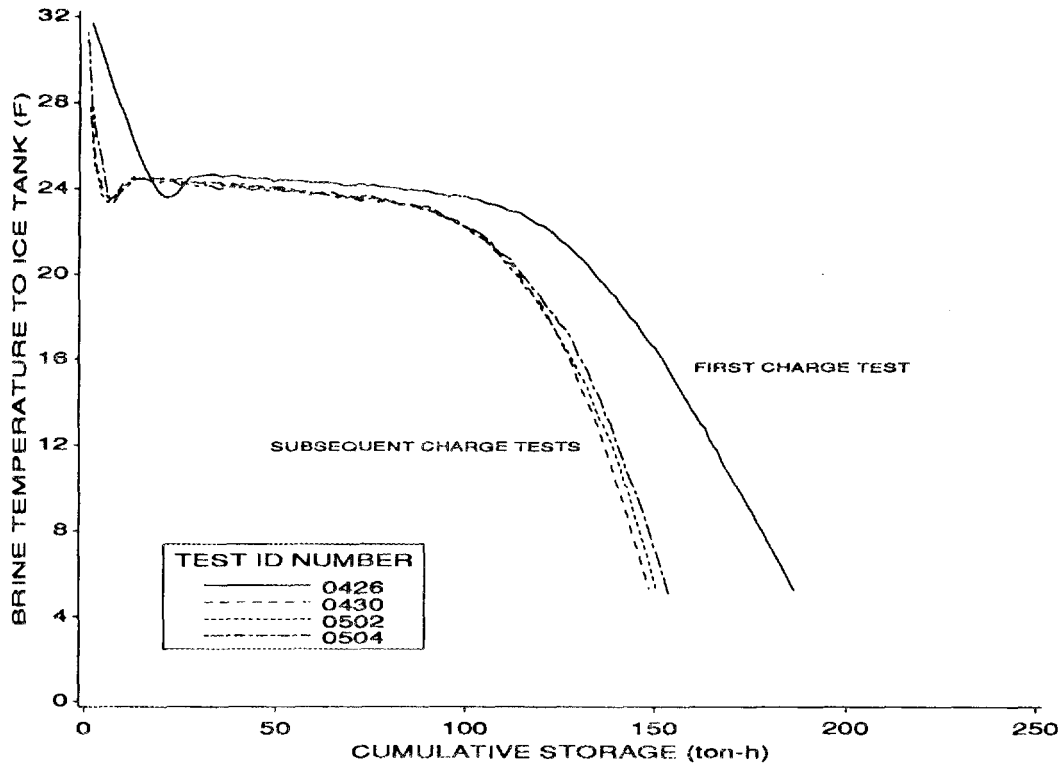


Fig. 6. FAFCO inlet brine temperatures show difference between initial and succeeding charge tests.

for tests with the approximate capacity of 18 tons and brine flows that vary from 50 to 150 gal/min. (The test at the highest flow rate began with a fully melted tank). Figure 9 shows the mean brine temperature in the ice tank, i.e. the average of the brine inlet and outlet temperatures, for these same tests. The difference between the brine inlet temperatures for the 50 and 150 gal/min tests is $\sim 6^{\circ}\text{F}$ (Fig. 8), while the difference between the average brine temperatures is only about 3°F (Fig. 9). Theoretically, this average brine temperature should be strictly a function of capacity and the heat exchanger design, with the flow rate controlling the difference between the brine inlet and outlet temperatures.

The variation of the inlet brine temperature with capacity is seen more clearly if tests with the same brine flow rate are compared as is shown in Fig. 10. The flow rates for these tests were between 108 and 123 gal/min. As shown on Fig. 10, the brine inlet temperature ranged from a low of $\sim 18^{\circ}\text{F}$ at 30 tons to a high of $\sim 25^{\circ}\text{F}$ at 15 tons.

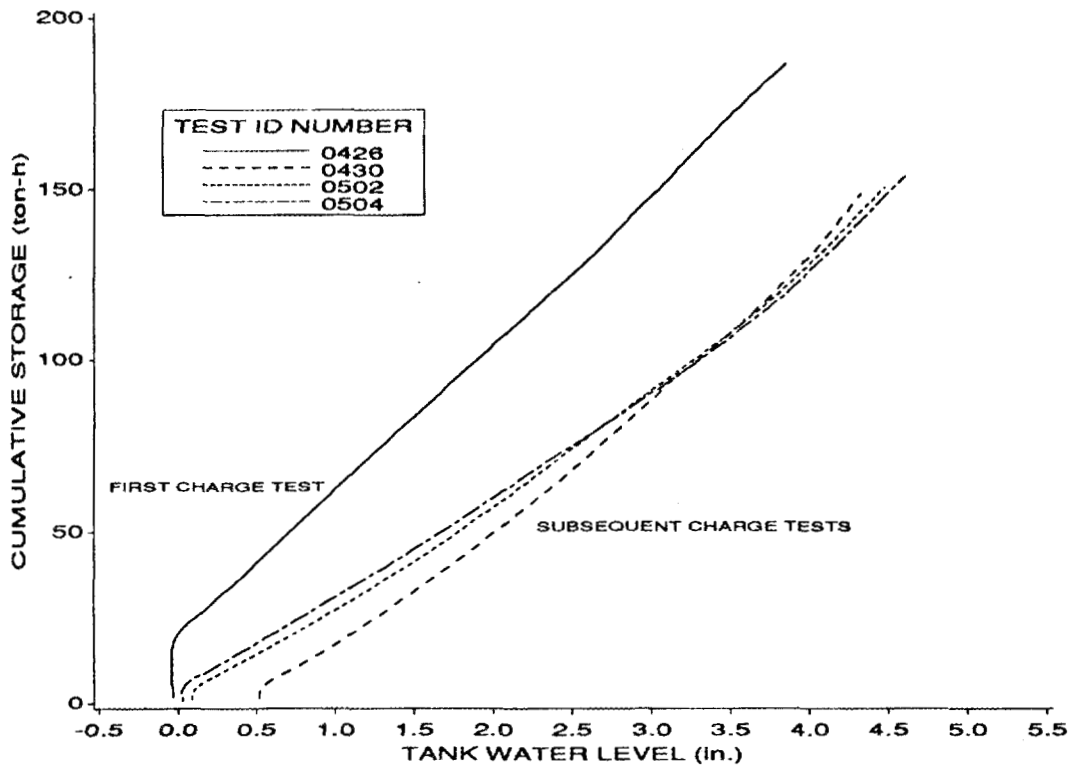


Fig. 7. Effect of pre-test conditions on tank water level indicator.

To aid customers in selecting the proper chiller, FAFCO provides the minimum brine temperatures to the ice tank during charge cycles of varying capacities and flow rates. The FAFCO values vary from 20 to 26°F, with the lowest values for the highest charge rates and lowest brine flow rates¹. A portion of the manufacturer's table, corresponding to ISTF test conditions, is shown in Table 3. The brine temperatures measured at the ISTF were significantly lower than these predicted temperatures. For example, FAFCO predicts that an 18 ton charge with a flow rate of 119 gpm should have a minimum entering brine temperature of ~24°F. However, as shown in Fig. 10, the plateau temperature for this test was slightly less than this value, with a minimum temperature of ~5°F. Comparison of Tables 2 and 3 shows that the **average** brine inlet temperature for almost every test was less than FAFCO's predicted **minimum** brine inlet temperature range. Figure 11 shows that if the tests had been stopped at the end of these plateaus, or when these manufacturer's

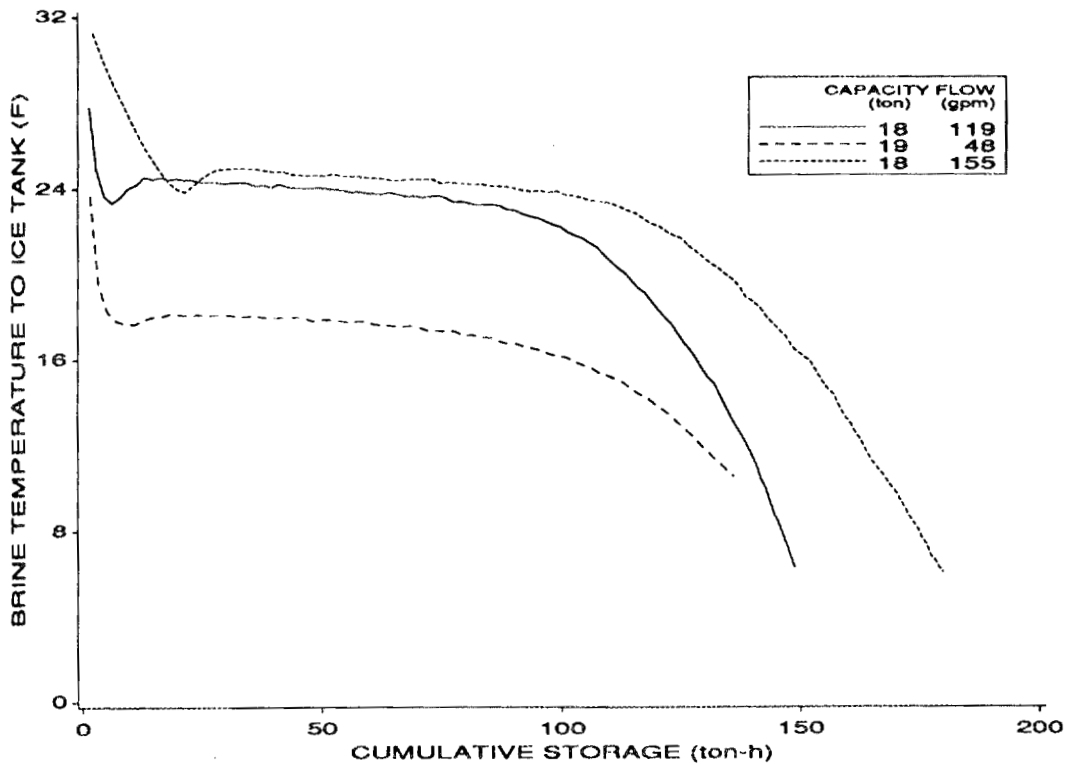


Fig. 8. Effect of brine flow rate on tank inlet temperature during FAFCO charge tests.

predicted minimum brine temperatures were reached, a significant portion of the stored energy would not have been charged and therefore the energy available for discharge would have been much less.

Traditional packaged chiller data provide adequate guidance when selecting equipment for constant temperature systems, such as air conditioners, but are less useful for ice storage systems. Figure 12 shows data that are typically available for a packaged chiller/condensing unit. The catalog data usually give the capacity as a function of condensing temperature and brine outlet temperature for a given range of brine temperature changes. Correction factors for brine concentration are also given or can be obtained from the manufacturer. In Fig. 12, the catalog data (shown as stars) for water chilling have been extrapolated to temperatures commonly encountered when making ice. Such extrapolations must be checked with the chiller manufacturer. The test data were examined to find a

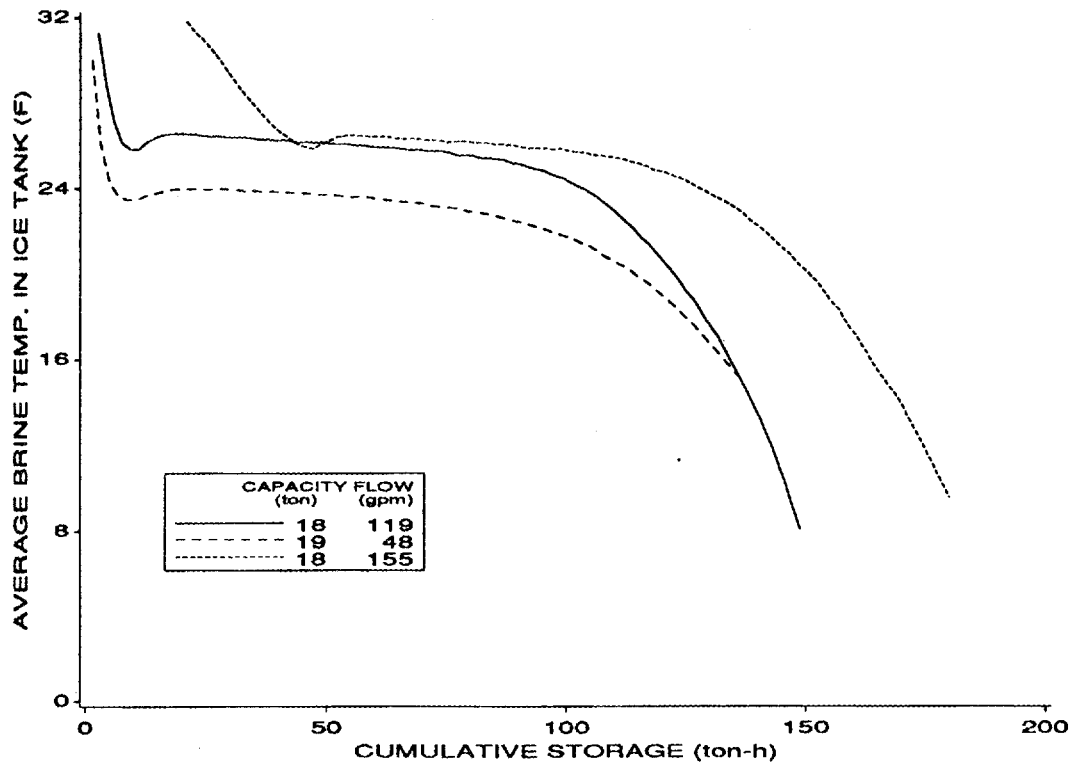


Fig. 9. Variation in average (of inlet and outlet) brine temperature during FAFCO charge tests over a range of brine flow rates.

method of predicting overall system performance, given variable load temperatures and this type of chiller data based on a constant load temperature.

The ISTF data were therefore correlated with tank state-of-charge, relative to a latent charge of 150 ton-h. This latent tank charge level was chosen based on the repetitive test results shown in Fig. 6. The results should be useful for tanks of similar design but with different storage capacities. The correlations were based on test data from those tests that started with some ice already present in the tank, as these are more representative of typical operating conditions. Only one test for each set of capacity/brine flow rate conditions was used to avoid weighing the results toward the conditions used for the repetitive tests shown in Fig. 6. The solution was broken into two regions to better reflect the temperature profiles seen in Fig 11. Equations (16) and (17) express the brine inlet temperature as a function of the capacity, the tank state of charge, and the brine flow rate. Equation (16) explained

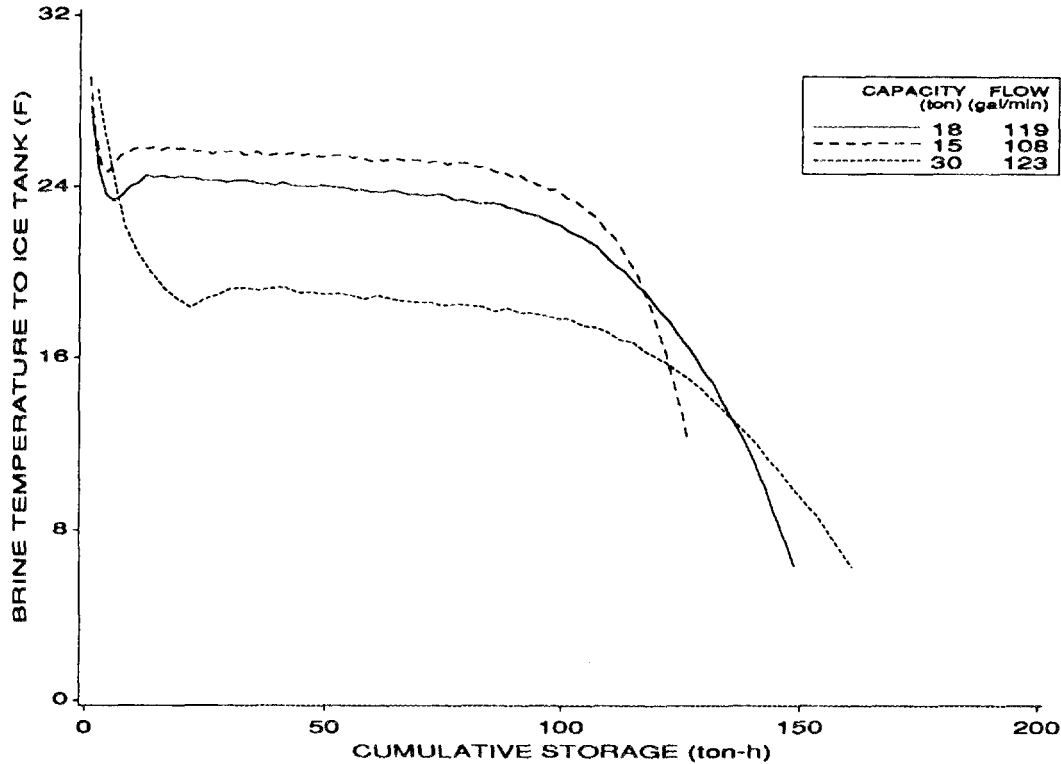


Fig. 10. Brine inlet temperature affected by charging rate during FAFCO charge tests.

~96% of the data variation, based on the adjusted squared correlation coefficient, and all the parameter estimates were significant at >99%, based on the Student's T-test. This equation can be interpreted as indicating that the brine inlet temperature decreases $\sim 0.42^{\circ}\text{F}$ for each increase of 1 ton in the capacity, decreases about 0.05°F for each percent increase in the tank charge (i.e., drops $\sim 0.5^{\circ}\text{F}$ as the tank goes from 60 to 70% charged), and decreases proportional to the inverse of the brine flow rate. Two of these parameters offset each other, because the capacity drops as the tank charge increases. Recalling that the capacity is approximately constant as the tank charge increases from 20 to 70% (see the linear portion of Fig. 4), this equation predicts that the brine inlet temperature would drop $\sim 2.1^{\circ}\text{F}$. This agrees well with the trends shown on Fig. 11. Equation (17) had an adjusted squared correlation coefficient of 66% and shows that during the latter portion of the charge cycle

Table 3. FAFCO charge sizing table, brine flow rates (gpm)

Charge Rate (ton)	Minimum Brine Inlet Temperatures (°F)					
	20.0	21.2	22.4	23.5	24.7	25.9
10						42
11						52
12					44	66
13					58	79
14				46	72	93
15				61	86	107
16			43	75	100	120
17			57	89	114	134
18			71	103	128	148
19		50	86	118	142	161
20		62	100	132	156	
21	46	75	115	146		
22	58	88	129	160		
23	69	101	144			
24	80	113	158			
25	92	126				
26	103	139				
27	114	152				
28	126	165				
29	137					
30	148					
31	160					

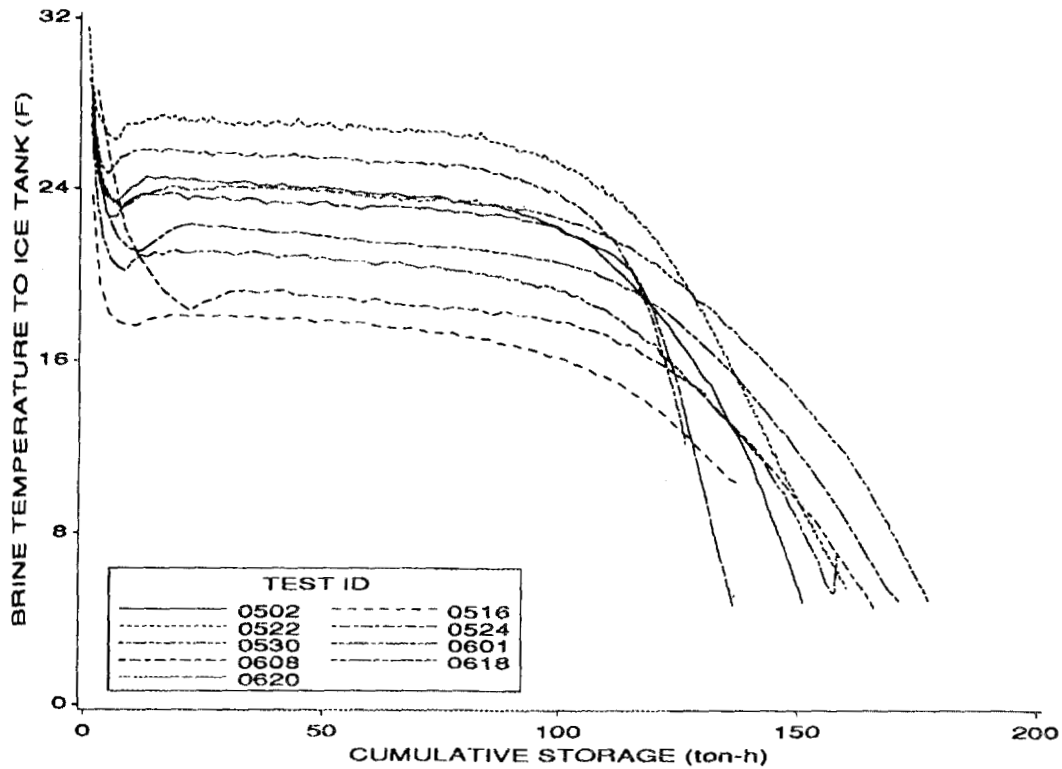


Fig. 11. Brine inlet temperature profile vs. cumulative energy storage during FAFCO charge tests.

the brine inlet temperature is much more sensitive to the amount of ice in the tank. While the brine inlet temperature dropped only about 0.5°F as the ice tank went from 60 to 70% charged, it drops $\sim 4^{\circ}\text{F}$ from 70 to 80% charged.

for $20\% < \text{SC} < 70\%$:

$$\text{TE16} = 37.7 - 0.42 \times \text{Re}_b - 0.047 \times \text{SC} - \frac{397}{\text{FE}^4}, \quad (16)$$

for $70\% < \text{SC} < 100\%$:

$$\text{TE16} = 53.3 - 0.16 \times \text{Re}_b - 0.42 \times \text{SC} - \frac{72.6}{\text{FE}^4}, \quad (17)$$

where

- TE16 = tank brine inlet temperature (°F),
 Re_o = refrigeration effect, or capacity (ton),
 SC = state of charge (%), and
 FE4 = brine flow rate (gal/min).

Equation (18) expresses the charging capacity as a function of the brine inlet temperature, the tank state of charge, and the brine flow rate. This equation is only valid for tank state of charge between 20 and 70% and has an adjusted squared correlation coefficient of 96%. As the tank becomes more fully charged, the charging rate dropped steeply for fast charge tests (at rates greater than 25 tons) but much more gradually for slow charge tests, as was seen in Fig. 3. Correlations in this region (>70% charged) were unable to account for more than 34% of the variation in charging rates and are not reported here.

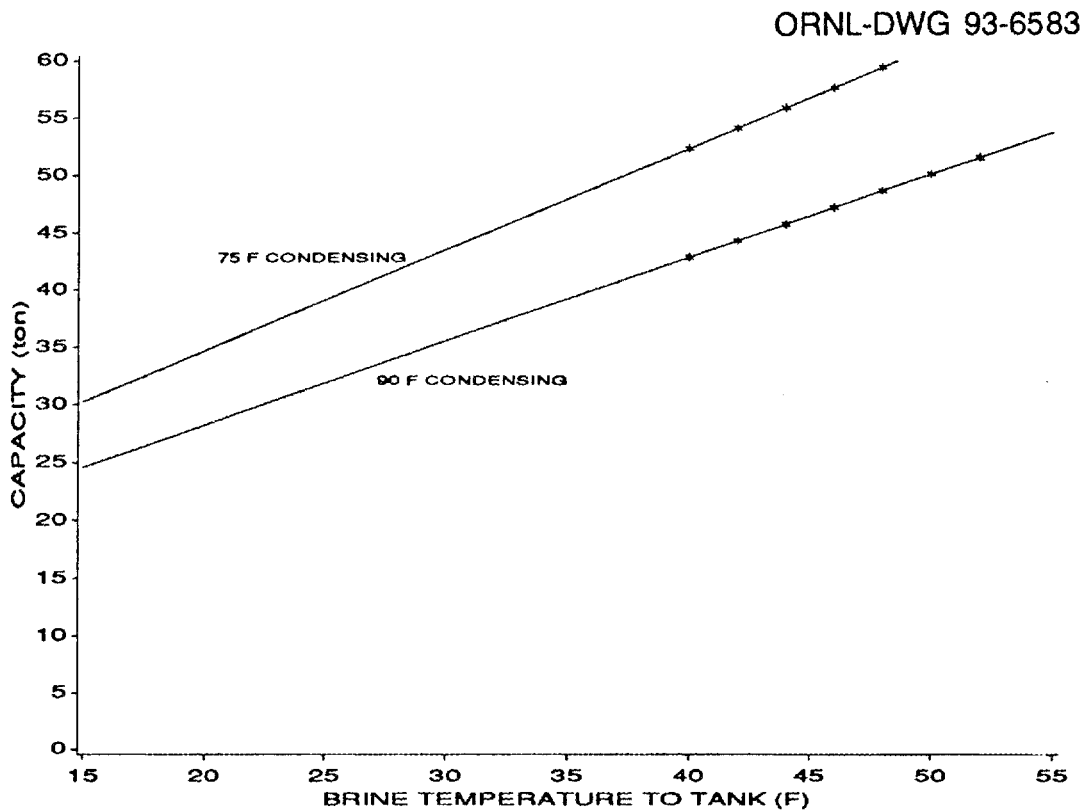


Fig. 12. Typical chiller/condensing unit performance curves.

However, this correlation did produce statistically significant (> 99% confidence) parameter estimates that show the charging rate is four times more sensitive to the state of charge than in Eq. (18) for the region from 20 to 70% charge.

$$\text{for } 20\% < SC < 70\%: \quad Re_b = 87.5 - 2.3 \times TE16 - 0.109 \times SC - \frac{928.}{FE4} \quad (18)$$

Together, these correlations show that the tank's typical charge behavior is relatively constant until the tank reaches about 70% of the full charge. After that point, both the charging rate and brine inlet temperature will quickly drop. To account for this, the designer

ORNL-DWG 93-6566

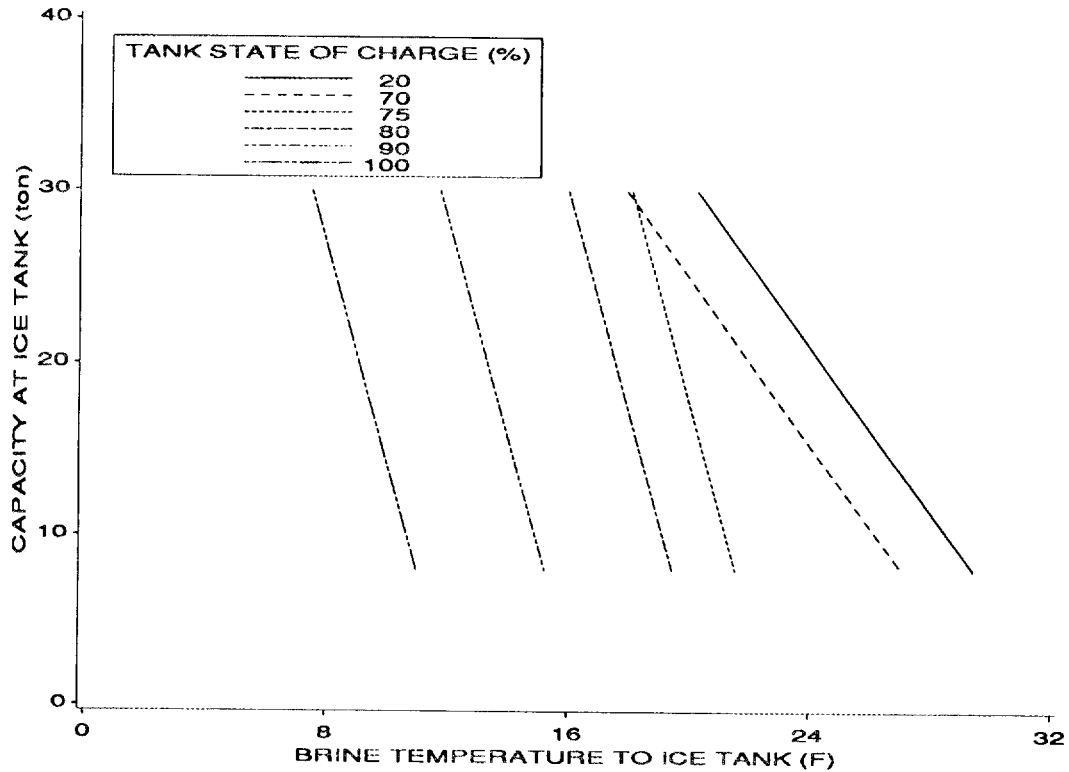


Fig. 13. Graphical depiction of Eqs. (16) and (17) of the relations between charging rate, brine inlet temperature, and tank state of charge for a brine flow rate of 100 gpm.

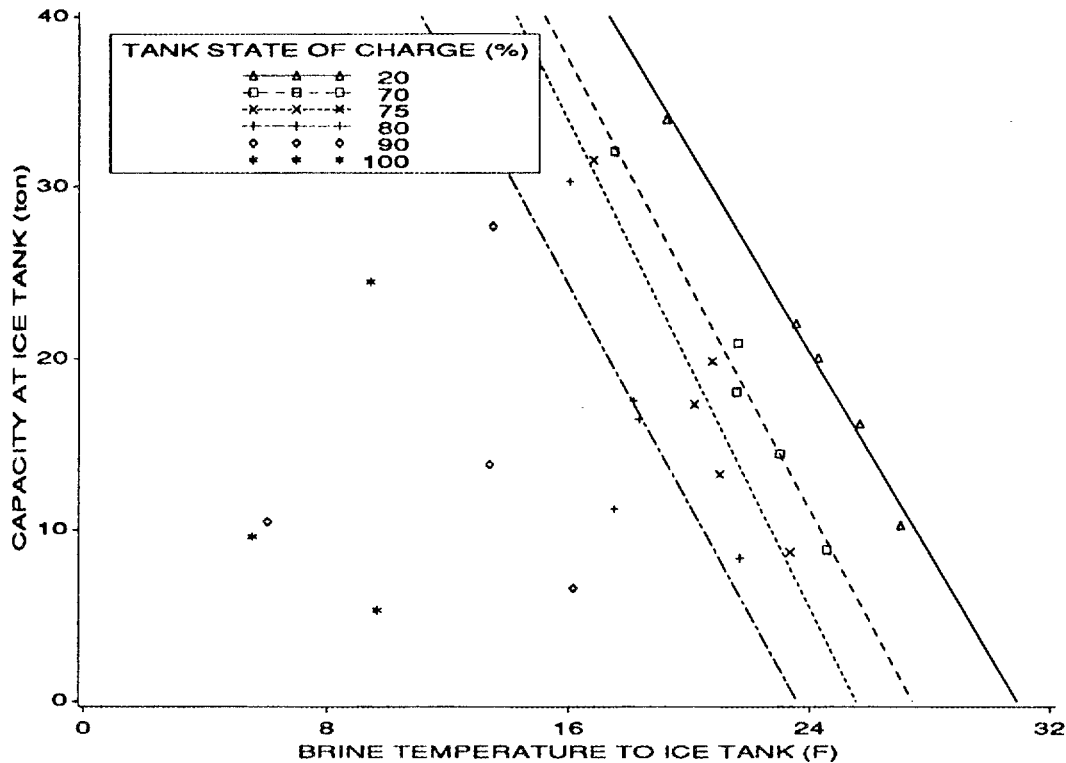


Fig. 14. FAFCO charge test data for brine flow rates between 78 and 125 gpm showing relationship between charging rate, brine inlet temperature, and tank state of charge.

must either: (1) specify excess ice storage capacity to keep the chiller conditions in the more constant range as the necessary ice is charged in the tank, or (2) select a chiller able to meet this profile (i.e., oversize the chiller), or (3) allow additional charging time at the reduced capacity.

Figure 13 shows the results from Equations (16) and (17) for a flow rate of 100 gpm. This can be compared to Fig. 14 which shows test data for those tests with flow rates between 78 and 125 gpm. Either of these figures can be used to assess the range of operating conditions that the chiller must experience during a charge cycle. A system designer, knowing the condensing temperature, brine concentration, and brine flow rate, can choose the appropriate chiller data and overlay this curve on Fig. 13. The result is shown in Fig. 15 where the solid line is the chiller performance curve. The system performance

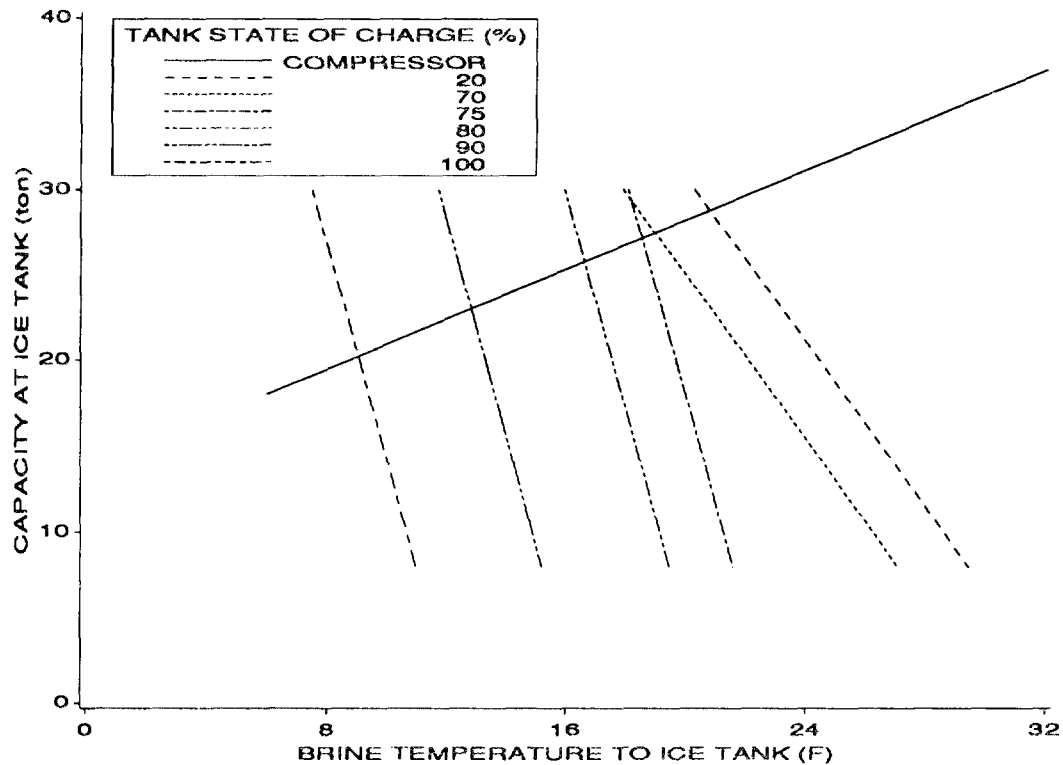


Fig. 15. Intersection of chiller performance and storage system performance parameters.

will be found at the intersections of the chiller data and the ice storage tank data. These values can be used to more precisely estimate the time necessary to charge the tank, especially if the tank charge begins from a partially frozen state. Figure 4 can also be used to estimate charging time. The changing slopes of the cumulative storage curves in Fig. 4 would correspond with the intersections between the capacity lines and the appropriate compressor curve, as demonstrated in Fig. 15.

The only auxiliary power requirement for the system in the charging mode is the brine pump. The pump power ranged from ~0.5 kW at 50 gpm to ~6 kW at 150 gal/min. If a 30-ton compressor was running at the higher flow rate with a compressor power consumption of 1.2 kW/ton, this additional power use and heat addition (assuming that the pump power is converted to heat in the brine, thereby reducing the available cooling capacity) would increase overall power consumption to ~1.5 kW/ton, an increase of ~23%.

At the lower flow rate for the same example case, the additional power use and heat addition would increase overall power consumption to ~ 1.22 kW/ton, an increase of $\sim 2\%$. If the system capacity was defined to be 30 tons to the load (i.e., pumping heat addition is not considered), then the higher flow rate case would have an overall power consumption of 1.4 kW/ton (a 17% increase) and the lower flow rate example would have an overall power consumption of 1.22 kW/ton (a 1% increase).

5.3 DISCHARGE PERFORMANCE

The ISTF simulates a building load with a simple resistance heater. This portion of the test loop was designed to model serving a constant load while maintaining constant inlet and outlet temperatures to the load. This is accomplished by recirculating a portion of the brine from the heater outlet to the heater inlet, bypassing the ice tank. During the course of the discharge test, the brine temperature leaving the ice tank gradually rises and this recirculation steadily decreases until the brine exiting the ice tank is at the desired heater inlet temperature. After that time, the desired heater outlet temperature is maintained by increasing the brine flow through the heater/ice tank loop. The test is considered completed when it is no longer possible to increase the brine flow and the heater outlet temperature exceeds the desired value. Typical FAFCO installations have been built with a different control method. FAFCO typically maintains a constant brine flow rate through the ice tank, rather than through the load. A variable portion of the flow bypasses the load to meet the constant demand with a constant load outlet temperature. The inlet temperature to the load is therefore uncontrolled and equals the ice tank outlet temperature. The ISTF piping arrangement was unable to mimic this control method. However, tests were made with a constant flow through the ice tank as in the FAFCO recommended system to investigate whether this would increase the available cool storage capacity. For these tests, the brine flow rate and heater power were held constant, there was no brine recirculation, and the brine temperatures were uncontrolled. These tests were considered to end when the ice tank outlet temperature reached 48°F. All the discharge tests are summarized in Table 4.

Table 4. FAFCO discharge test summary

Test Number	Average Capacity (Ton)		Heater Outlet Temperature (°F)		Tank Outlet Temperature (°F)	Average flow To Ice Tank (gpm)	Average Flow to Heater (gpm)	Average Pump Power (kW)
	Heater	Tank	Planned	Average Measured				
0427	25	26	60	59	36	30	53	0.4
0501	25	26	60	60	39	33	54	0.4
0503	25	26	60	60	39	32	53	0.4
0509	25	27	60	60	39	32	53	0.4
0521	37	41	60	60	43	56	79	0.8
0523	25	26	50	50	38	60	64	0.8
0529	25	26	55	55	41	54	71	0.8
0531	19	19	50	50	38	46	51	0.6
0604	20	21	NC	44	40	159	158	6.2
0607	19	19	60	60	40	26	40	0.3
0615	19	18	55	55	41	41	54	0.5
0619	35	33	55	55	40	72	92	1.2
0621	35	29	NC	50	44	159	158	6.2
0626	25	24	60	60	43	45	51	0.5
0628	26	21	NC	47	42	159	158	6.2
0924	24	25	60	60	40	34	52	0.4
0926	24	25	60	60	40	34	52	0.4
0928	24	25	60	60	40	34	52	0.4
1002	26	26	NC	47	42	111	110	2.3

As mentioned in Sect. 4.3, the discharge capacity was measured at both the heater and the ice tank. The measurement at the heater should be slightly less than the measurement at the ice tank because of heat gains by the circulation pumps. Temperature measurement errors of $\pm 0.5^{\circ}\text{F}$ (for tests 0427-0628) or $\pm 0.2^{\circ}\text{F}$ (for tests 0924-1002) can also occur at any of the four monitoring points used to calculate the change in water temperature across the tank and heater. The total discharge energy measured at the ice tank was compared to the sum of the total measured at the heater plus the pump energy. These two values matched within 5% for 70% of the tests. For the other tests, the ice tank measurement was always significantly lower (by 7 to 27%) than the heater measurement. Comparison of these results to other test data, including heater control settings, indicates that

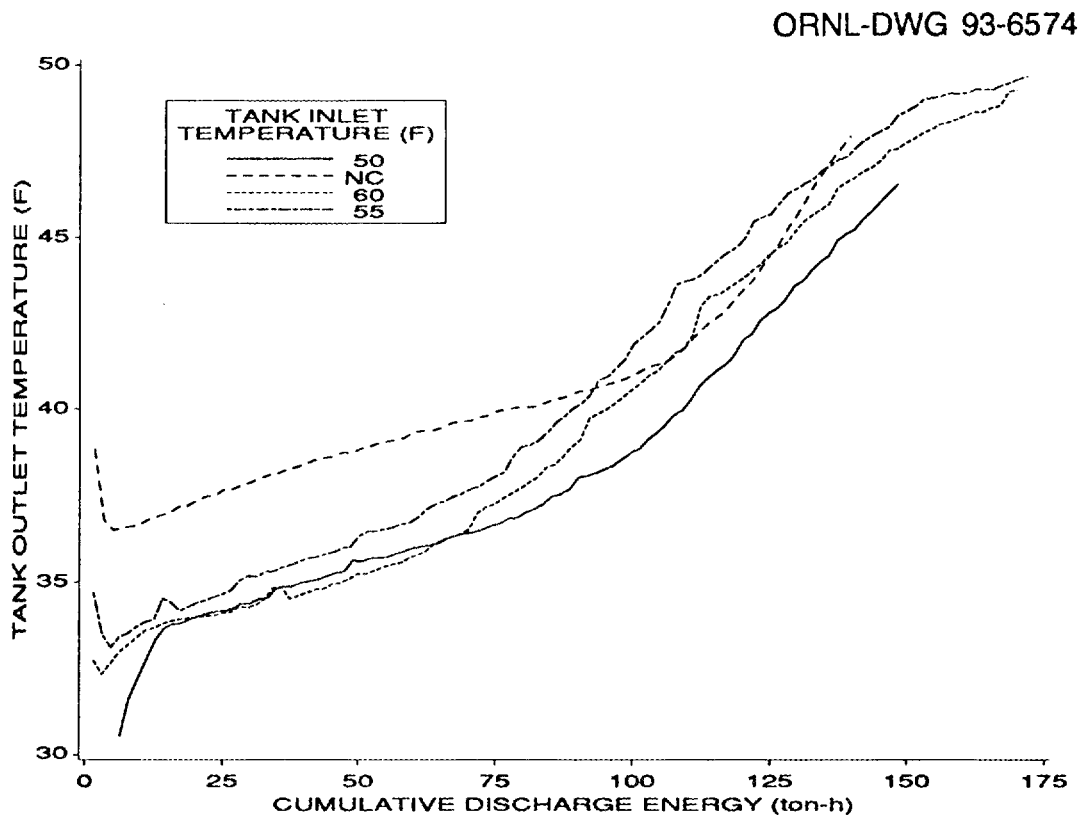


Fig. 16. Ice tank outlet temperature variation for constant discharge rate of 19 tons with controlled tank inlet temperature from 50 to 60°F. One test is included with no temperature control but with a constant brine flow rate of 158 gpm.

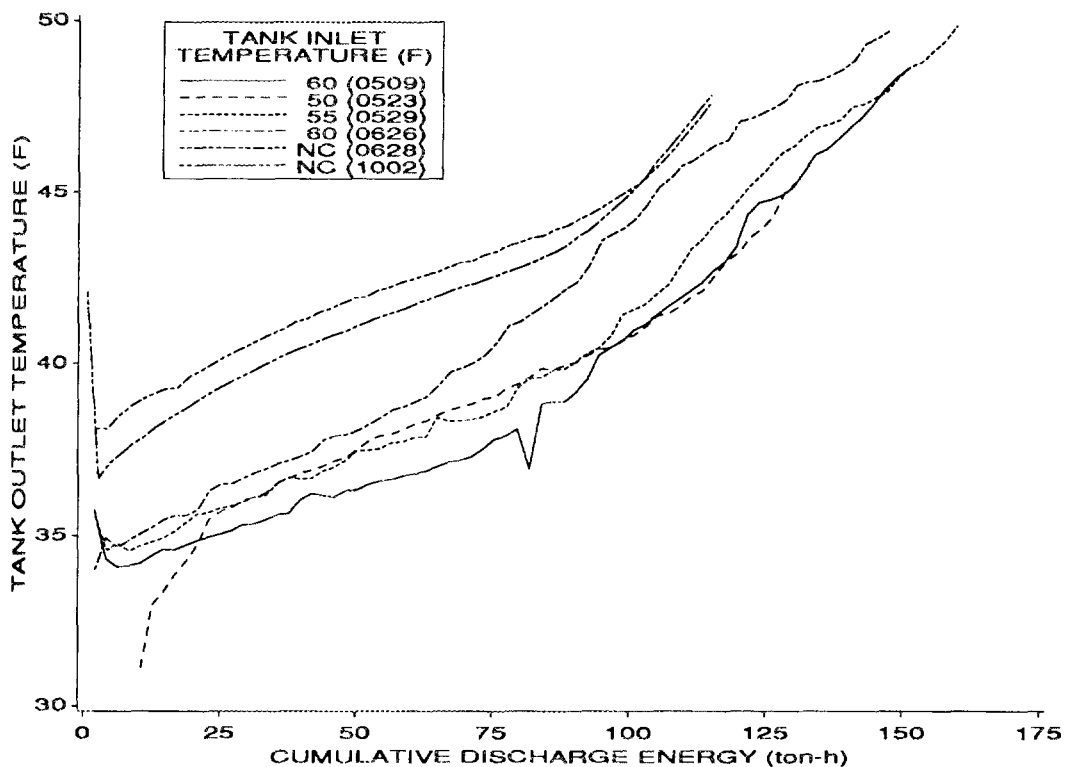


Fig. 17. Ice tank outlet temperature variation for constant discharge rate of 25 tons with controlled tank inlet temperatures from 50 to 60°F. Two constant brine flow rate tests are also shown.

the capacity calculations at the heater are more reliable. Therefore, all capacity data presented in this section are based on Eq. (14).

The water temperature leaving the ice tank varied according to the discharge rate and the water temperature entering the tank. Figures 16 - 18 show the discharge temperature profiles vs the cumulative discharge energy. These figures demonstrate that the tank outlet temperature slowly but steadily rises from about 35°F to 50°F after the first 25 ton-h are harvested from the tank. The initial shape is affected by the tank's immediate history. Some discharge tests began directly after the previous charge test was completed. For these tests, the initial brine temperature was as low as 5°F. Other tests began after the tank rested overnight. For these tests, the initial brine temperature usually was around 32°F, representing the equilibrium temperature of a tank of frozen water. Figure 16 shows 4 tests

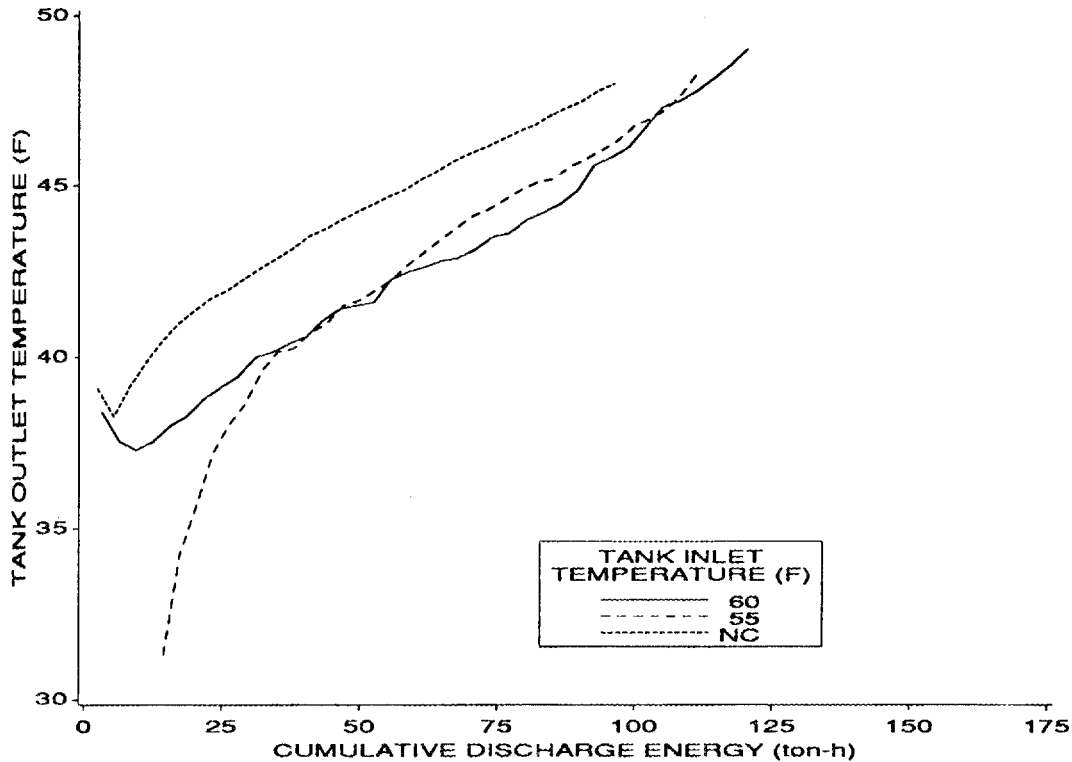


Fig. 18. Ice tank outlet temperature variation for constant discharge rate of 35 tons with controlled inlet temperature of 55 and 60°F. One test at a constant brine flow rate of 158 gpm included.

made with a constant discharge capacity of 19 tons. There is little difference in the temperature profiles as the tank inlet temperature varies from 50 to 60°F. However, the test run at a constant brine flow rate and no inlet temperature control shows a higher overall outlet temperature and a smaller total cooling capacity, only 140 ton-h vs 170 for the case where the inlet temperature was maintained at 55°F. The same trend can be seen in Fig. 17 for tests run at a constant load of 25 tons. Here, those tests with uncontrolled temperatures and higher constant flow rates were only able to provide 115 ton-h of cooling, while the test with an inlet temperature of 50°F provided 130 ton-h of cooling and those with inlet temperatures of 55-60°F provided about 150 ton-h. Figure 18 shows the much steeper temperature rise associated with a higher discharge rate of 35 tons. Here, again, the higher

constant flow rate produced the least cooling, 95 ton-h vs 120 ton-h for the 60°F inlet temperature test.

As Figs. 16 to 18 have shown, the total cool storage available depends on the discharge rate, the control strategy, and the maximum allowable inlet temperature to the load. This availability was explored by noting the cumulative discharge energy at the times when the ice tank outlet temperature reached 40 and 44°F and at the end of the test. This relationship should be useful to a system designer who knows the length of the on-peak period, the total load to be met, and the maximum temperature to the load that will provide adequate comfort and dehumidification. Equations (19) and (20) were the result of this examination for the controlled temperature and constant brine flow tests, respectively. Both equations show high adjusted correlation coefficients, 0.98 for Eq. (19) and 0.99 for Eq. (20). All the parameter estimates were significant at higher than 99% confidence as measured by the Student's t-test. Equation (19) predicts the total discharge energy within $\pm 10\%$ for controlled temperature discharges of 75 ton-h or more and within $\pm 5\%$ for discharges of 130 ton-h or more. Equation (20) predicts the total discharge energy for constant flow rate tests within $\pm 5\%$.

$$\sum \text{cap}_h = -173. + 2.48 \times \text{TE14} + 15.2 \times \tau \times e^{\frac{12 - \tau}{12}} + 2.02 \times \text{cap}_h, \quad (19)$$

$$\sum \text{cap}_h = -151. + 3.81 \times \text{TE14} + 10.3 \times \tau \times e^{\frac{12 - \tau}{12}}, \quad (20)$$

where

$\sum \text{cap}_h$ = cumulative discharge capacity measured at the heater (ton-h),

τ = time from start of discharge test (h),

TE14 = brine temperature leaving the storage tank (°F), and

cap_h = constant discharge capacity at heater (ton).

These equations show the available discharge energy to be a function of both discharge rate and maximum allowable tank outlet temperature for controlled heater

temperatures and of tank outlet temperature only for constant brine flow, as is shown in Figs. 19-21. The curves represent the maximum discharge energy available in a given time period for the specified discharge rate or tank outlet temperature. The curves' generated using Eqs. (19) and (20) have a slope that becomes less as time increases. However, all discharge tests were run at a constant discharge rate, which would give a constant slope. To avoid projecting the curves from Eqs. (19) and (20) beyond their logical applicability, their end points were chosen to be that point where the calculated cumulative capacity was equal to 90% of the product of the discharge rate and the elapsed time. Figure 19 shows both ISTF data and curves from Eq. (19) for a maximum tank outlet temperature of 48°F with discharge rates from 19 to 35 tons. Figure 20 provides the same information for a discharge rate of 25 tons and maximum heater outlet temperatures from 40 to 52°F. Equation (20) was used to generate the curves shown Fig. 21. A discharge rate of 25 tons

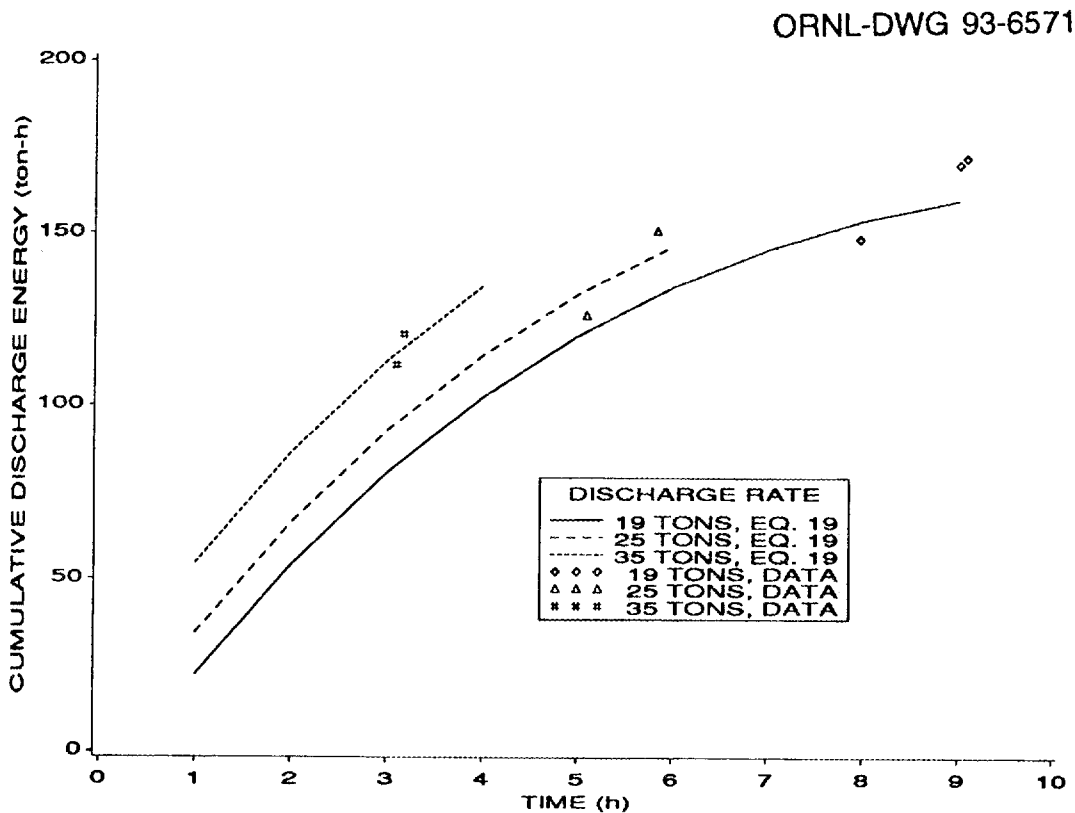


Fig. 19. Available discharge energy vs. time for loads from 19 to 35 tons and a maximum brine temperature of 48°F with controlled heater temperatures.

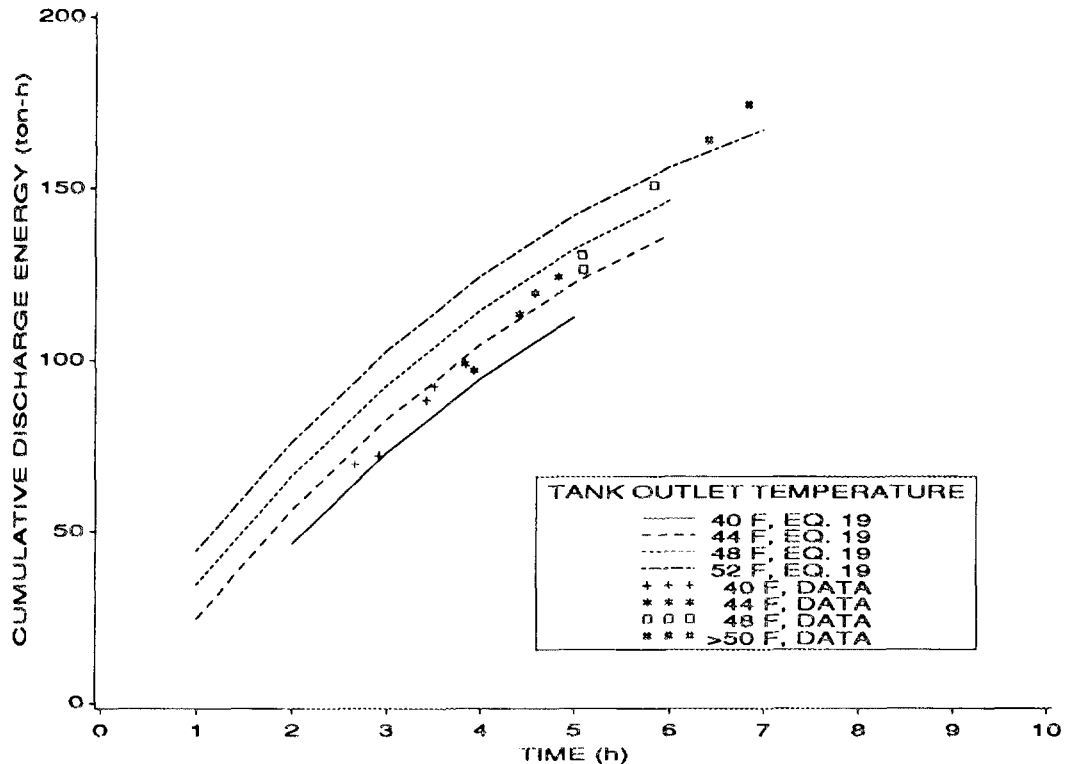


Fig. 20. Available discharge energy vs. time for maximum brine temperature from 40 to 52°F and a load of 25 tons with controlled heater temperatures.

was used to select the end points of these curves (based on the 90% cutoff previously described), although the discharge rate is not used in the equation. The ISTF data on this figure show that further extrapolation may be appropriate for the uncontrolled temperature condition of Eq. (20).

Power requirements during discharge include brine pumping power. The pumping power varies with the brine flow rate and ranged from 0.4 to 6.2 kW. This accounted for an approximate heat input to the brine of between 0.5 to 12 ton-h over the course of the discharge cycle, assuming that all the pump power is converted to heat in the brine.

5.4 STANDBY HEAT GAINS

Standby heat gains were measured in a test that spanned a period of 30 days. Visual observation confirmed that all ice was below the water surface at the beginning and end of

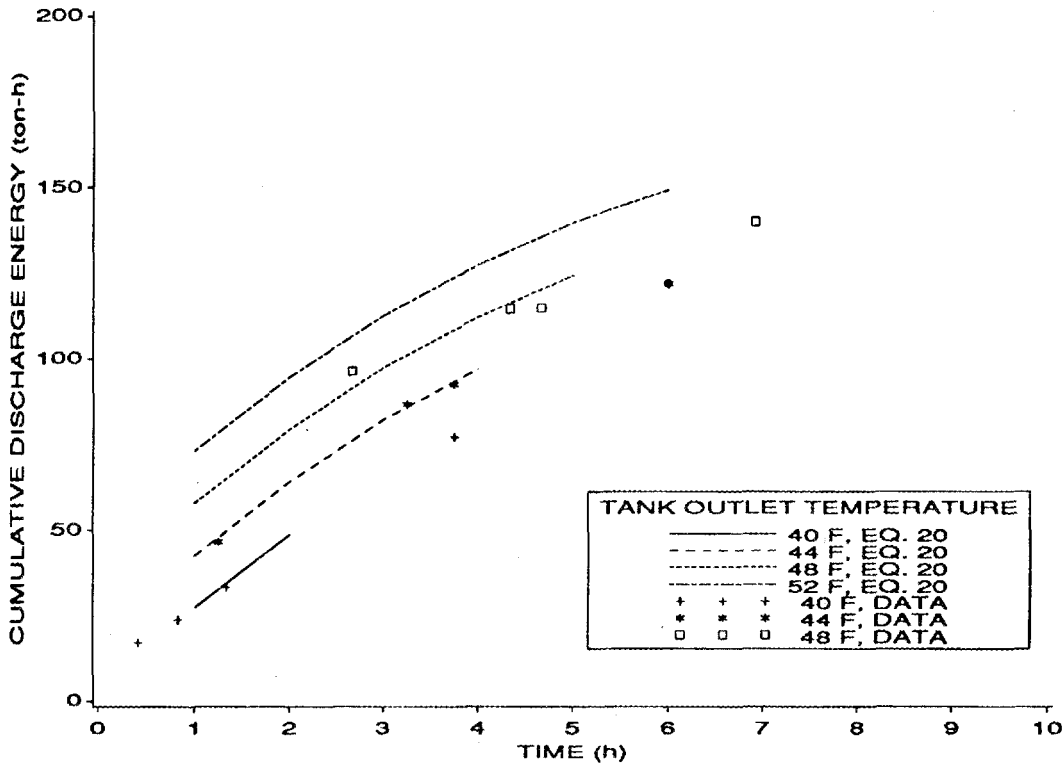


Fig. 21. Available discharge energy vs. time for maximum brine temperatures from 40 to 52°F for constant brine flow to the ice tank.

this period. The change in tank depth, with the measured ice density of 57.2 lb/ft² and an ice heat of fusion of 144 Btu/lb, gave the latent heat gain for the tank containing ice. This calculation assumes that all the water in the tank remains at 32°F, which is reasonable considering the large and well-distributed ice inventory throughout the test. Over a period of 704 h, the tank lost a total of 73 ton-h of ice, corresponding to a standby loss rate of 0.1 ton. Based on the repetitive storage capacity of 150 ton-h, this loss rate can be expressed as 0.0007 ton/ton-h, or alternatively, it would take 1500 h (63 d) for a fully charged tank to melt. The ambient temperature throughout this test remained between 65 and 85°F, and there was no direct sunlight upon the tank.

Using FAFCO's reported insulation value of R-15 and an assumed temperature difference of 40°F, the heat gain rate would be 0.09 ton, very close to the measured value of 0.1 ton.

6. CONCLUSIONS AND RECOMMENDATIONS

The FAFCO ice storage system tested was consistently able to manufacture and store between 150 and 200 ton-h of ice. This was true for a wide range of charging rates and brine flow rates. The discharge capacity varied from 80 to 170 ton-h and was heavily dependent upon the discharge conditions, including discharge rate and brine temperature requirements. The unit showed consistent repeatability, low pressure drops, and low jacket losses. Piping connections and controls were simple and the unit was leak-free.

The amount of capacity variation during a charge cycle was greatest for the higher charge rates. This can have significant effects on the equipment performance and should be a primary factor in equipment selection. Therefore, variations in operating schedules could affect the charging performance for a given chiller system. The discharge performance was also strongly dependent upon the tank discharge rate and tank outlet temperature. These parameters must therefore be clearly specified before the storage tank selection is made. Changes in the discharge schedule or required temperature after installation can alter the available discharge energy.

REFERENCES

1. FAFCO Manufacturing Corporation, Ice Stor Product Information Manual, FAFCO Inc., Redwood City, California, January 1990.
2. T. K. Stovall and J. J. Tomlinson, *Commercial Cool Storage Laboratory Test Procedure*, ORNL/TM-11511, Martin Marietta Energy Systems, Inc., Oak Ridge Natl. Lab., May 1990.
3. G. T. Kartsounes and R. A. Erth, "Computer Calculation of the Thermodynamic Properties of Refrigerants 12, 22, and 502," *ASHRAE paper No. 2200*, presented at ASHRAE Annual Meeting, Washington D.C., August 22-25, 1971.
4. *UCARTHERM Heat Transfer Fluid*, Union Carbide Corporation, Industrial Chemicals Division, Danbury, Conn., 1986.
5. P. V. Hobbs, *Ice Physics*, Clarendon Press, Oxford, 1974.
6. F. M. White, *Viscous Fluid Flow*, McGraw-Hill Book Co., New York, 1974, pp. 484-485.
7. Electric Power Research Institute, *Commercial Cool Storage Design Guide*, EM-3981, Palo Alto, Calif., May 1985.

Appendix A

ISTF INSTRUMENTATION

A.1 DATA ACQUISITION AND CONTROL

A data acquisition system and computer are used to control the thermal loading rate, the brine and refrigerant circulation pump speeds, recirculation valve positions, and the condensation temperature and to collect the data from system instrumentation. The computer allows short sampling times of the instrumentation to provide data for detailed analysis and feedback during transient system operation. Direct controls, outside of the data acquisition/computer system, are available for compressor loading, booster pump operation, and auxiliary portions of the test facility.

A.2 TEMPERATURE MEASUREMENTS

Refrigerant temperature measurements are made by RTDs bonded to the outside of the copper pipes. These RTDs were calibrated by the manufacturer to 0.3°F . After installation, the recorded refrigerant temperatures were compared to the expected thermodynamic states for the corresponding pressure measurements. Water and brine temperature measurements are made by RTDs inserted into the PVC pipes. These RTDs are calibrated by the manufacturer to $\pm 0.5^{\circ}\text{F}$ and are checked against an ice bath after installation. The RTDs were also checked against each other under conditions where an unloaded heat exchanger, for example, would be expected to show the same inlet and outlet temperature. The RTD calibrations are periodically rechecked, and instruments that have drifted beyond 0.5°F are replaced. The RTD's used for water and brine measurements were upgraded during the course of the FAFCO tests. The new RTD's are calibrated to $\pm 0.2^{\circ}\text{F}$.

A.3 FLOW MEASUREMENTS

Vortex-shedding flowmeters are used to measure the condenser cooling water flow, the water/brine flow to the heater, the water/brine flow to the ice tank, and the gaseous

refrigerant flow to the condenser. The vortex-shedding refrigerant flowmeter imposes a pressure drop of ~ 0.5 psia. These flowmeters are accurate to $\pm 0.8\%$ of the reading for liquid flows and $\pm 1.5\%$ of the reading for gaseous flows. The flowmeters used to measure water and brine volumetric flow were checked after installation by running water through the lines into a 55-gal drum placed on a scale.

The Coriolis mass flowmeters used to measure liquid refrigerant mass flows to the low-pressure receiver, the ice tank, and the thermal expansion valves were calibrated by the manufacturer to $\pm 0.4\%$ of full scale, which is 1000 lb/min. A sight glass is positioned to provide a visual confirmation of single-phase flow downstream of the meter. These Coriolis flowmeters are very difficult to calibrate after installation because of the closed nature of the refrigerant system. However, the volumetric flow through one of the vortex-shedding flowmeters can be compared to the mass flow through one of these Coriolis meters. Also, energy balances on the condenser, low-pressure receiver, chiller/evaporator, and ice tank can be used to assess the continued accuracy of these devices.

A.4 PRESSURE MEASUREMENTS

Refrigerant pressure measurements are made with pressure transducers to allow the electronic recording of the values. The accuracy of these absolute pressure readings is rated at $+0.11\%$ of full scale. However, the calibration certificates supplied with each transducer show accuracies of $\pm 0.004\%$ or better. Also, the transducer calibration was rechecked after installation and periodically thereafter using laboratory calibration equipment. The pressure transducers located in the high-pressure portion of the loop, that is, between the compressor discharge and the expansion valve, are rated for 0 to 500 psia. All others are rated for 0 to 250 psia. During testing, the pressure measurements are periodically compared to other measurements within the loop and to the expected refrigerant properties.

A differential pressure meter can be used to measure the change in tank water depth during charging. The meter measures from 0 to 10 in. of water with an accuracy of $\pm 0.5\%$ of full range output (i.e., ± 0.05 in. of water).

A.5 ELECTRICAL MEASUREMENTS

Electrical measurements for the compressor power (rated at 40 and 75 hp), circulating pump(s) power (from 2 to 5 hp), agitation air compressor power (1/2 hp), and heater power (0 to 135 kW) are measured by watt/watt-hour transducers. The watt-hour measurements are accurate to $\pm[(0.2\% \text{ of the reading} + 0.01\% \text{ of the rated output})/(\text{power factor})]$. The watt-hour meters for the compressors were checked by measuring the voltage and current on each of three phases. The watt-hour meter for the heater was checked by comparison to the heat absorbed by the water as measured by the flow and temperature change. The accuracy of this heater's watt-hour meter is poor because of the semiconductor-controlled rectifier (SCR), or phase-angle power controller, used to vary the heater power. Heater energy use measurements are therefore based on the fluid flow rate and temperature change, although the power consumption is recorded as an additional check.

A.6 COOL STORED MEASUREMENT

The change in storage medium volume is used to measure the amount of expansion due to ice formation for ice on coil systems. The amount of ice formation, along with the sensible heat removed from the storage medium indicates the quantity of cool stored in the tank. The differential pressure transducer described in a previous section was mounted at the initial water level in a section of tubing that was immersed in the tank at one end and fixed to a vertical support at the other.

Appendix B

CMA TESTS IN FAFCO TANK

B.1. SCOPE AND PURPOSE OF TESTS

When calcium magnesium acetate (CMA) is mixed with water, the freezing point of the water is lowered. Calcium magnesium acetate could therefore be used to provide cool storage at temperatures below 32°F. Also, CMA has been identified as altering the structure and adhesion qualities of ice. It might therefore effect the heat transfer in an internal-melt intermediate fluid ice storage system.

A mixture of about 7% (by weight) of CMA and water was placed in the FAFCO tank. This mixture should have a freezing point between 27 and 28°F. A series of charge and discharge tests were then made. The discharge tests were patterned after tests previously performed on the FAFCO tank when filled with plain water. The charge tests were chosen to span a range of charging rates. Because the charging rate is affected by the suction temperature, it was not possible to exactly match charge tests with CMA to previous charge tests.

B.2. TEST CONDITIONS

The charge tests made with the CMA solution are summarized in Table B.1. Several tests made previously with plain water are also included in this table for comparison and they will be discussed later in this section.

The discharge tests are summarized in Table B.2. As closely as possible, the CMA solution tests duplicated previous tests made with plain water. However, two difficulties affected the ability to start the discharge tests with the same amount of cool storage available to meet the load. First, as water freezes in the CMA solution, the remaining solution becomes more concentrated and its freezing point is further depressed. The freezing temperature of the heat transfer fluid therefore became a limiting factor in the amount of ice that could be frozen. When the minimum brine temperature of 0°F was reached during the

Table B.1. FAFCO charge tests, CMA experiments

Test ID	Compressor Loading (hp/%)	Condensing temperature (°F)	Brine flow rate (gpm)	Average capacity (tons)	CMA present
1022	40/100	90	113	17	yes
1024	40/50	95	117	8	yes
1026	75/100	93	115	26	yes
1031	40/75	94	115	17	yes
1107	40/100	90	50	13	yes
0504	40/100	90	118	18	no
0524	40/75	90	108	15	no
0608	75/100	90	123	30	no
0613	40/75	90	105	14	no
0620	40/100	100	107	20	no

CMA charge tests, the amount of ice in the tank was much less than it was during previous tests with plain water. Second, during previous tests with plain water, the depth of the water in the storage tank was used as an indication of the amount of ice stored at the end of a charge cycle. This was possible because all the ice was submerged, solidly built up around the heat exchanger tubing. However, with CMA in the tank, there was a certain amount of free-floating ice that made this measurement inaccurate. Also, as will later be discussed, the density of the CMA solution in the tank tended to produce stratification, introducing further errors when the density of the fluid in the tubing used to measure the fluid depth no longer equaled the density of the solution in the tank. It therefore became difficult to ascertain the amount of ice present within the tank.

Table B.2. FAFCO discharge tests, CMA experiment

Test ID	CMA	Heater inlet temperature (°F)	Heater outlet temperature (°F)	Capacity (tons)	Cumulative discharge energy ^a (ton-h)
1023	yes	47	59	24	107
427	no	48	59	25	132
1025	yes	48	59	17	107
607	no	48	60	19	124
1030	yes	48	58	34	85
521	no	48	60	37	84
1102	yes	41	55	18	90
531	no	40	50	19	133
1108	yes	NC ^b	NC	16	86
604	no	NC	NC	20	118

^aAs measured by the brine at the heater from the test start until the tank outlet temperature reaches 44°F

^bNC = not controlled

B.3 RESULTS

When the CMA mixture was initially frozen, the brine inlet temperature dropped below 16°F before the first ice crystals were seen. As Fig. B.1 shows, the brine temperature at the onset of freezing varied from about 14 to 22°F during the CMA tests. Figure B.2 is a plot showing comparable tests from the FAFCO unit before the CMA was added to the tank. These tests were chosen for comparison because they were made with similar brine flow rates, similar compressor loading and condensing temperatures. The capacity is not however exactly the same because the CMA ice froze at a colder temperature, affecting the

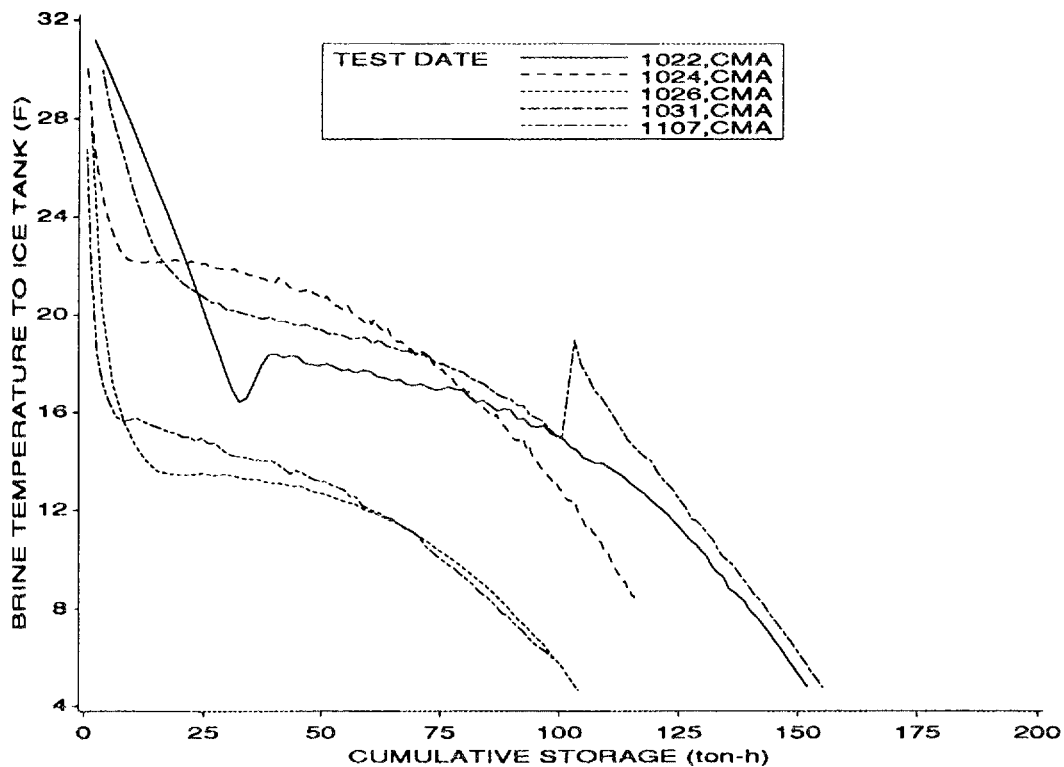


Fig. B.1. Brine inlet temperature during CMA freeze tests.

brine temperature in the chiller and therefore lowering the evaporating temperature. In these previous tests, the brine inlet temperature usually showed the start of freezing at about 24°F.

When the ice began to form in the tank, it was first noticeable as small soft granules on the tubes very near to the surface of the water. These granules could not be felt at a depth of about 6 in. below the surface of the water. Next, soft slushy ice appeared floating between the banks of tubes, starting about 8 in. away from the tank sides and continuing through the tank. At this time, soft ice could be felt on all the inlet tubes. It was quite soft and came free of the tube at the slightest touch. Then small blobs/flakes of ice about 1/2 in. in diameter came floating to the surface. When a small area of the surface was cleared, more of these flakes could be seen rising from below. The surface temperature at this point was a little below 29°F. After almost 2 h of freezing, the slush on the tubes was noticeably stiffer, but was still soft at its outer edges and the tube could still be cleared with a bare

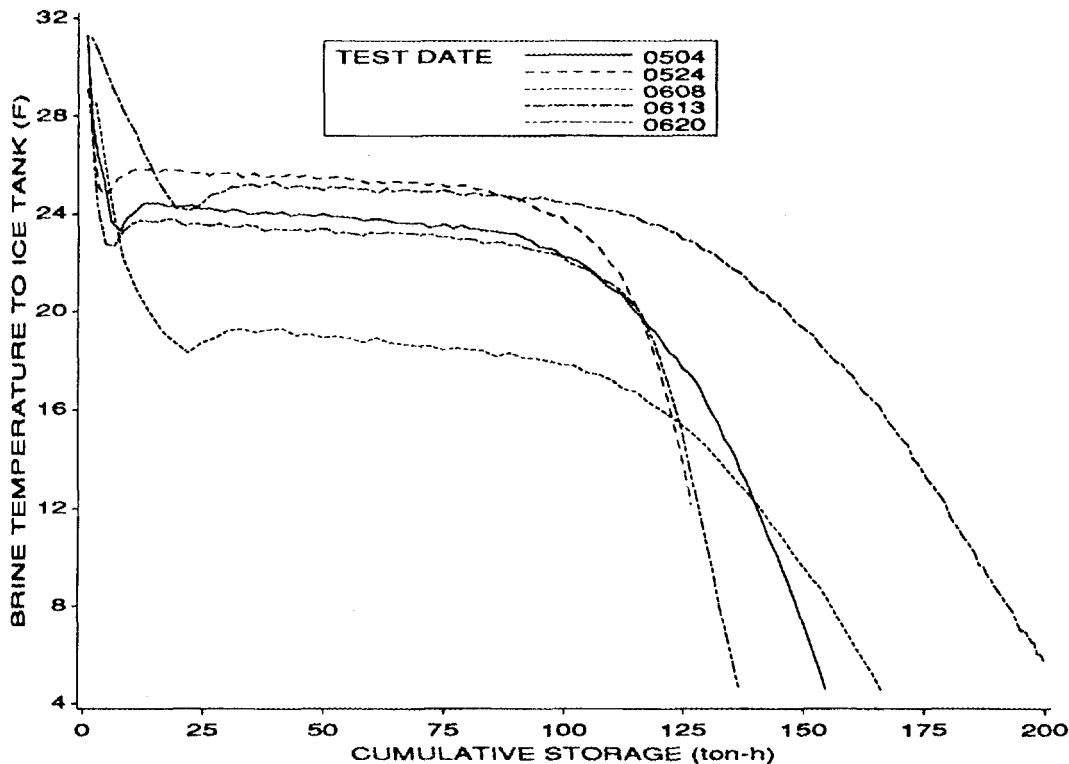


Fig. B.2. Brine inlet temperatures during non-CMA freeze tests.

hand pushing gently on the ice. After sitting for a 2-day period the ice was nearly as hard as ice made without CMA, although a fingernail could be pressed into the ice.

Before the first test, the CMA mixture was well mixed within the tank using air agitation. During the initial test, there was a lot of white flock present in the water. During later tests, this material appeared to have settled out and could be seen resting on the tube supports and spacers. The water was then quite clear.

After a discharge cycle, a cap of crumbly ice, about 3 - 4 in. thick, hung above the water. This cap appeared to be slightly thinner near the center of the tank.

After almost two weeks of tests (including four complete freeze and melt cycles), a sample of the tank contents was taken at the surface and found to have a specific gravity of 1.000. A sample taken 4 in. below the surface had a specific gravity of 1.001 and a sample taken from the bottom of the tank had a specific gravity of 1.082. The tank was then mixed

using air agitation. Samples from both the bottom and the top then showed a specific gravity of 1.041. The next morning, top and bottom samples showed the same specific gravity of 1.040. After one freeze/melt cycle was completed, the sampling procedure was repeated and showed the specific gravity 6 in. above the tank bottom to be 1.055 and the specific gravity at the top to be 1.024. Sixty hours later (and at a slightly higher temperature) the specific gravity at the top was 1.020 and the bottom specific gravity was 1.054. This lack of change indicates that the stratification is not due to simple settling within the tank. It appears that when the ice freezes and floats to the top, it brings pure water with a lower density to the top of the tank, thereby causing the significant stratification in density and CMA concentration. This theory was further confirmed when a chunk of ice was broken from the ice cap hanging above the water level. When this ice chunk was melted, it had a specific gravity of 1.001, showing that very little CMA was present in the ice. A tank using CMA would therefore need to be equipped with some method of agitation to remix the solution on a periodic basis.

After the first three freeze/melt cycles were completed, two thermocouples were placed in the tank, one located 6 in. above the bottom and the other 3 in. below the surface of the solution in a fully-melted tank. The T/Cs agreed within 0.1°F in an ice bath before placement in the FAFCO tank. Figure B.3 shows the difference between the top and bottom temperatures recorded at these locations during two freeze/melt cycles. Because the first cycle was done following three freeze/melt cycles, the CMA solution was stratified within the tank, but the tank was well mixed when the second cycle began. The well mixed freeze and melt processes display mirror image profiles. During the freeze process the top of the tank was initially warmer than the bottom, but during the course of freezing the tank, the two temperatures became equal. The well mixed melt process shows the opposite behavior, with the top and bottom beginning at nearly equal temperatures, but with the top becoming warmer as the ice melted. The freeze and melt cycle made with the stratified tank showed quite different behavior. The top temperature was significantly lower than the bottom temperature throughout the stratified freeze process. Again, the melting process showed the

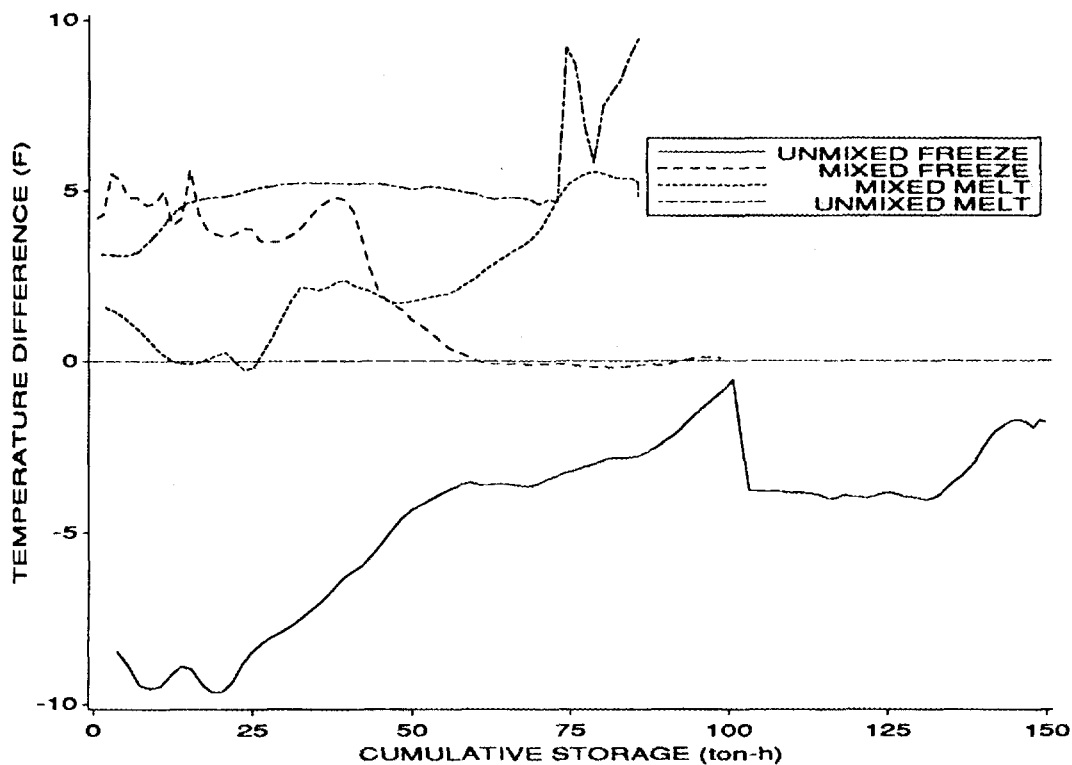


Fig. B.3. Difference between tank top and bottom temperatures (i.e., $T_{top} - T_{bottom}$) affected by CMA distribution within tank.

opposite behavior. During the stratified melt test, there appeared to be a sharp rise in the surface temperature near the end of the test. It is possible that the T/C near the top of the tank became exposed to the air when the water level sank during melting, because a portion of the tank's contents would have been located in the hanging ice cap, causing the water height to be less than it was initially, when the T/C was placed 3 in. below the water surface in a fully melted tank.

As Figs. B.1 and B.2 show, the total energy storage capacity of the tank was greatly decreased by the addition of CMA. The amount of this derating is a function of the refrigeration plant and the freezing point of the intermediate heat transfer fluid. However, even if lower charging temperatures were available, it would be necessary to limit the

portion of the tank contents frozen to avoid saturating the remaining CMA solution. Therefore, independent of the refrigeration plant limitations, there will be some derating in any tank's storage capacity.

The temperature profiles of the brine leaving the ice tank during comparable discharge tests, with and without CMA are shown in Figs. B.4 and B.5. Figure B.4 compares tests made at a discharge rate of ~19 tons under varying brine flow rates. Figure B.5 makes a similar comparison for tests at faster discharge rates, from 25 to 37 tons. In these figures, all the tests with the CMA mixture are shown to reach the maximum brine outlet temperature before those without CMA. This is largely attributable to the smaller amount of ice made in the tank during the CMA freezing process. More importantly, both figures show the temperature rise occurring faster (i.e. with a sharper slope) for the CMA cases.

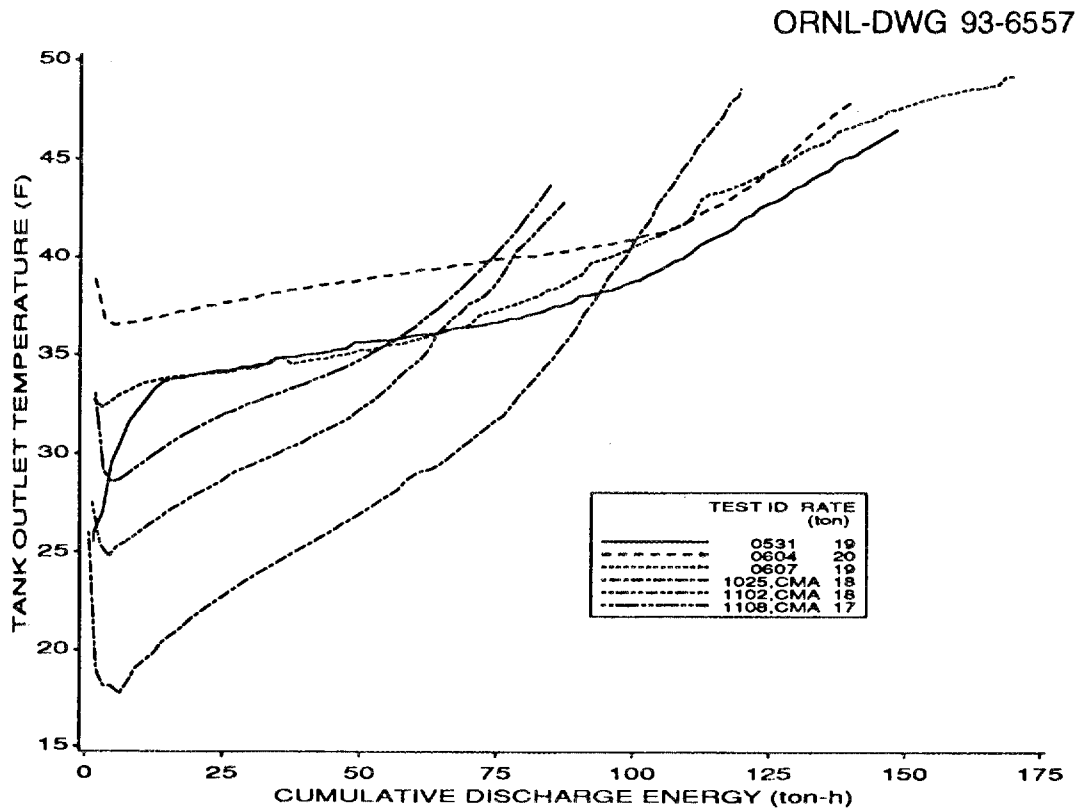


Fig. B.4. Comparison of tank outlet temperatures during discharge cycles with and without CMA.

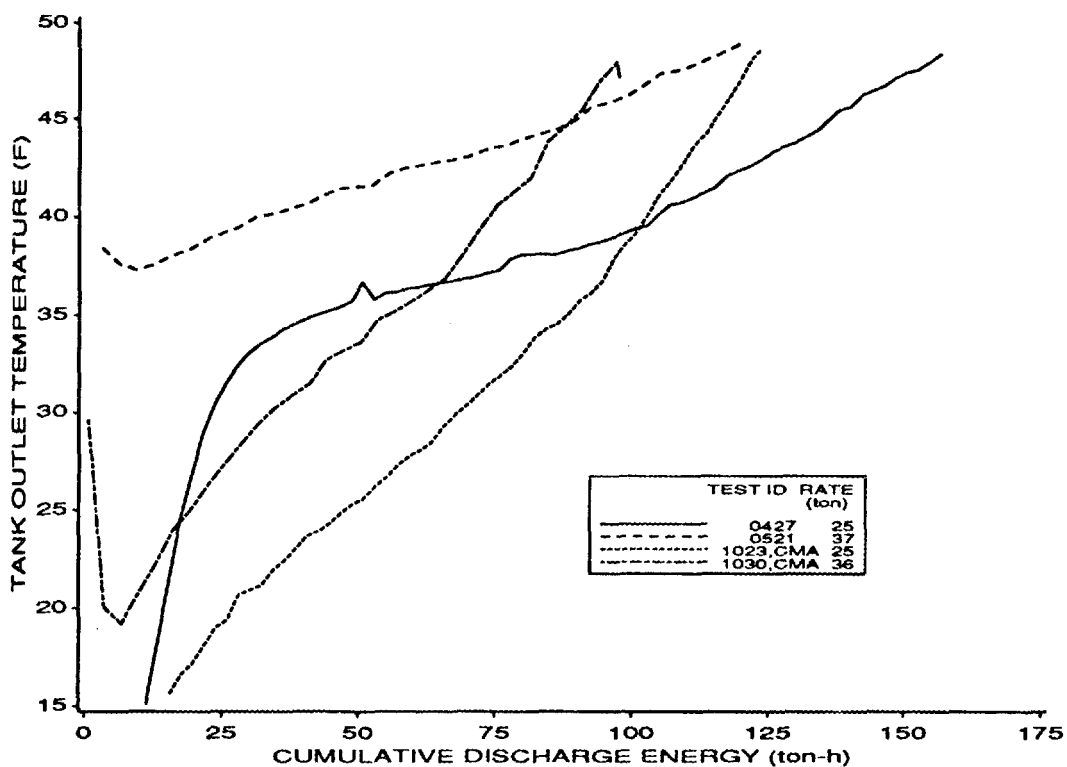


Fig. B.5. Comparison of tank outlet temperatures during faster discharge cycles, with and without CMA.

However, the reduced ice temperatures in the CMA tests led to a greater brine temperature change in the ice tank, and therefore a reduced brine flow rate. The brine flow through the ice tank for the five pairs of discharge tests considered here averaged 20% less for the CMA tests than for the tests with plain water. This will translate to reduced pumping power requirements and therefore an improvement in efficiency.

As discussed, the ice made with CMA was much softer than ice made with plain water. It was not known whether this softness was caused by entrained water (with a higher CMA concentration and therefore lower freezing point) or air, or by some other change to its crystalline structure. The effect of this softness on the unit's heat transfer properties was of great interest. It was hypothesized that water might be able to circulate within the ice, thereby enhancing the overall heat transfer by adding internal convective mechanisms to the conductance of the solid ice. Conversely, if entrained water was unable to circulate within

the soft ice structure, it could very well decrease the conductivity, since water's conductivity is only about 1/4 that of ice. If the softness is caused by minute air pockets, the conductivity would almost certainly decrease due to the poor conductivity of air, ~1/100 that of ice.

In order to quantitatively examine this issue, a 'UA factor' was calculated. The total heat transfer during a charge cycle can be expressed as

$$\text{cap}_t = U \times A \times (T_{\text{tank}} - T_{\text{brine}}) \quad , \quad (\text{B.1})$$

where

- cap_t = charging capacity measured at ice tank,
- U = overall heat transfer coefficient,
- A = total heat transfer surface area,
- T_{tank} = temperature of tank contents, and
- T_{brine} = temperature of brine.

The tank temperature, T_{tank} , is constant during most of the charge cycle, at 32°F for a tank full of water and at 28.6°F for a well-mixed tank of CMA and water. The brine temperature, T_{brine} , varies from the ice tank inlet to the outlet. The log mean temperature difference, frequently used for heat exchangers, is inappropriate here due to two factors that are contrary to the log mean temperature difference derivation: (1) the non-flowing nature of the water side of the heat exchanger and (2) the latent energy storage precludes the expression of the water-side's internal energy change in terms of its temperature. Therefore, a simple average of the brine inlet and outlet temperatures was used for the brine temperature in this equation. The heat transfer coefficient, U , combines the effect of forced convection on the inner tube surface, the conductivity of the heat exchanger tube, the conductivity of the ice adhering to the tube wall, and the effect of natural convection on the outer surface of the ice. The conductivity of the ice decreases almost linearly with the thickness of the ice on the coils. This will therefore cause the overall heat transfer coefficient to decrease as the ice inventory of the tank increases. The heat transfer area, A ,

increases proportional to the square of the ice thickness until the ice bridges between the heat exchanger tubes. This bridging causes a temporary decrease in the heat transfer area, which then grows much more slowly than the pre-bridging rate.

Due to this complex dependency of the UA product on the ice inventory, it is not possible to independently calculate the heat transfer coefficient of the softer CMA ice from the available performance data. However, the UA product can be calculated and is shown in Figs. B.6 and B.7 for charge tests with and without CMA, respectively. These results show the UA factor decreasing steadily for the CMA cases, with a consistently linear slope. Figure B.7 shows a completely different shape for the plain water tests, with an almost steady value throughout most of the tests, followed by a sharp decrease near the end of the charge cycle. The plateau is most likely attributable to the relative magnitudes of the increasing heat transfer area and the decreasing ice conductance (similar to the classical pipe insulation problem). The end of the plateau may represent the point at which the ice bridges

ORNL-DWG 93-6560

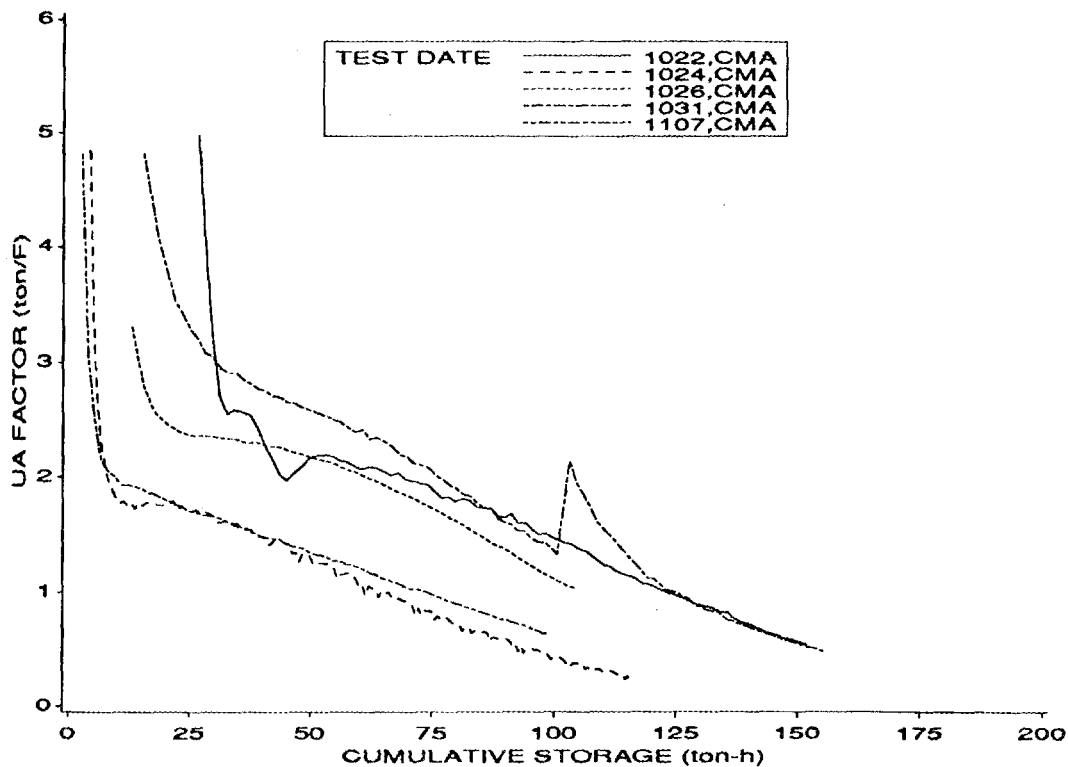


Fig. B.6. UA product for tests with CMA.

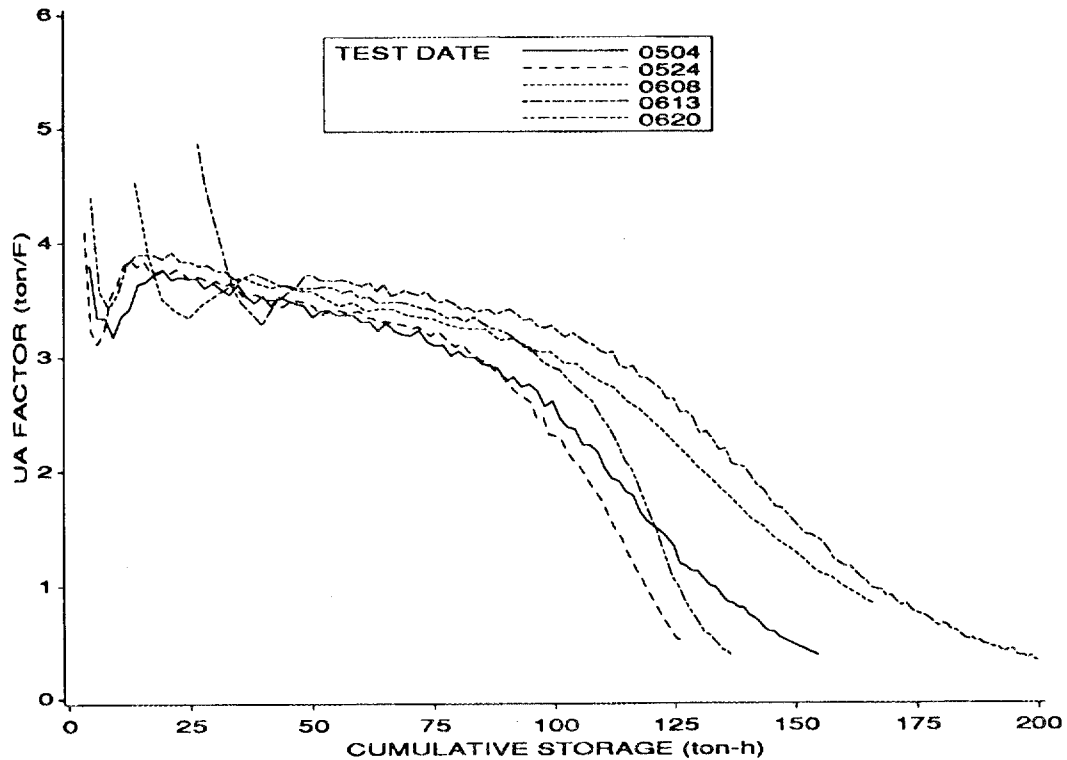


Fig. B.7. UA product for tests without CMA.

between coils and the surface area decreases. The average UA factor for the plain water cases was 70% higher than for the CMA cases. This would indicate that the softer CMA ice had a much lower conductance than plain ice, due either to entrained air or entrained water in stationary pockets. The shape of the CMA UA curves in Fig. B.6 indicates that the increasing surface area is unable to compensate for the increased heat transfer resistance as the ice thickness grows on the heat exchanger tubes.

The UA results show that the difference between the tank and average brine temperatures would have to be much greater for the CMA cases to achieve the same charging rate. Also, the tank temperature is lower for the CMA cases. The combination of these two effects demonstrates a need for much lower chiller temperatures, and hence lowered chiller efficiencies, for the CMA application. This result should preclude the use of CMA for heat exchanger surfaces where ice is allowed to build up.

B.4. CONCLUSIONS

The CMA lowers the tank storage temperature, enabling the application of ice storage to customer needs at lower temperatures. However, the tank outlet temperature rises much faster while melting the CMA ice, so that this advantage is limited to a relatively small portion of the stored energy. The CMA also decreases the total storage capacity of the tank compared to that of plain water. Also, while making ice, the inlet brine temperatures for the CMA mixture are much lower than for plain water due to the lower heat transfer characteristics of the CMA ice. This increases the efficiency penalty associated with lower ice-making temperatures. Periodic agitation of the tank contents would also be necessary to avoid CMA concentration stratification. Overall, the application of CMA in ice-on-tube ice storage systems was found to be of limited use.

Internal Distribution

- | | | | |
|-----|-----------------|--------|-------------------------------|
| 1. | T. D. Anderson | 15. | A. C. Schaffhauser |
| 2. | V. D. Baxter | 16. | M. Siman-Tov |
| 3. | S. H. Buechler | 17-26. | T. K. Stovall |
| 4. | R. S. Carlsmith | 27. | J. J. Tomlinson |
| 5. | W. G. Craddick | 28. | C. D. West |
| 6. | P. D. Fairchild | 29. | G. L. Yoder |
| 7. | D. J. Fraysier | 30. | ORNL Patent Section |
| 8. | W. Fulkerson | 31. | Central Research Library |
| 9. | R. B. Honea | 32. | Document Reference Section |
| 10. | J. E. Jones Jr. | 33-34. | Laboratory Records Department |
| 11. | L. Jung | 35. | Laboratory Records (RC) |
| 12. | W. A. Miller | | |
| 13. | W. R. Mixon | | |
| 14. | M. Olszewski | | |

External Distribution

36. Doug Ames, Transphase, Inc. 15572 Commuter Lane, Huntington Beach, California 92649
37. John Stephen Anderpont, Chicago Bridge & Iron Company, 800 Jorie Boulevard, Oak Brook, IL 60522-7001
38. John Bruce, Transphase, Inc. 15572 Commuter Lane, Huntington Beach, California 92649
39. Debra L. Catanese, P.E., Pennsylvania Electric Company, 311 Industrial Park Rd., Johnstown, PA 15904
40. Tom Carter, Baltimore Aircoil Company, P.O. Box 7322, Baltimore, MD 21227
41. Russ Eaton, Director, Advanced Utility Concepts Division, U.S. Department of Energy, Forrestal Building, CE-142, 1000 Independence Avenue, Washington, DC 20585
42. Freeman Ford, FAFCO, Inc., 2690 Middlefield Road, Redwood City, California 94063-3455
43. Imre Gyuk, Office of Energy Storage and Distribution, U.S. Department of Energy, Forrestal Building, CE-32, 1000 Independence Avenue, Washington, DC 20585

44. Landis Kannberg, Battelle Pacific Northwest Laboratories, P.O. Box 999, Battelle Boulevard, Richland, WA 99352
45. Don Kemp, Turbo Refrigerating Company, 1815 Shady Oaks Drive, P.O. Box 396, Denton, TX 76202
46. K. W. Klunder, Director, Office of Energy Management, Department of Energy, CE-14, Forrestal Building, 1000 Independence Avenue, Washington, DC 20585
- 47-96. Dave Knebel, Director of Research, Thermal Storage Applications Research Center, University of Wisconsin-Madison, 150 E. Gilman Street, Suite 1200, Madison, WI 53703-1493
97. George Manthey, DOE, Oak Ridge Operations, Oak Ridge, TN 37831
98. Robert P. Miller, Baltimore Aircoil Company, P.O. Box 7322, Baltimore, MD 21227
99. Tony Min, Mechanical Engineering Department, North Carolina Agricultural and Technical State University, Greensboro, NC 27411
100. Victor A. Needham III, Marketing Programs Director, Cincinnati Gas & Electric Company, P. O. Box 960, Cincinnati, Ohio, 45201.
101. Dave Pellish, U.S. Department of Energy, Forrestal Building, MS CE-332, Room 5H-79, 100 Independence Avenue, Washington, DC 20585
102. Veronika A. Rabl, Electric Power Research Institute, 3412 Hillview Avenue, P.O. Box 10412, Palo Alto, CA 94303
103. Eberhart Reimers, Advanced Utility Concepts Division, U.S. Department of Energy, Forrestal Building, CE-142, 1000 Independence Avenue, Washington, DC 20585
104. Tim Roddy, FAFCO, Inc., 2690 Middlefield Road, Redwood City, California 94063-3455
105. Richard Rhodes, FAFCO, Inc., 2690 Middlefield Road, Redwood City, California 94063-3455
106. Marwan Saliba, Energy Engineering Institute, Dept. of Mechanical Engineering, San Diego State University, San Diego, CA 92182-0191
107. Brian Silvetti, Calmac Manufacturing Corporation, Box 710, 150 South Van Brunt Street, Englewood, NJ 07631
108. Robert L. San Martin, Deputy Assistant Secretary, Office of Utility Technology, Department of Energy, CE-10, 6C-026/Forrestal Bldg., 1000 Independence Avenue, Washington, DC 20585
109. Chang W. Sohn, U.S. Army Corps of Engineers, P.O. Box 4005, Champaign, IL 61824-4005
110. Laura Thomas, Marketing Manager, York International Corporation, P.O. Box 1592, York, PA 17405-1592
111. Samuel G. Tornabene, Edison Electric Institute, 1111 19th Street, N.W., Washington, DC 20036-3691
- 112-136. R. D. Wendland, Electric Power Research Institute, 3412 Hillview Avenue, Box 10412, Palo Alto, CA 94303
137. Maurice W. Wildin, Professor, The University of New Mexico, Department of Mechanical Engineering, Albuquerque, NM 87131

- 138. Office of Assistant Manager for Energy Research and Development, Department of Energy, ORO, Oak Ridge, TN 37831
- 139-148. Given distribution as shown in DOE/OSTI-4500-R75 under Category UC-202 (Thermal Energy Storage)